MASS SPECTROMETRIC APPROACHES TO PROBING THE REDOX FUNCTION OF APE1

Sarah Ann Delaplane

Submitted to the faculty of the University Graduate School
in partial fulfillment of the requirements
for the degree
Master of Science
in the Department of Biochemistry and Molecular Biology,
Indiana University

July 2011

Accepted by the Faculty of Indiana University, in partial
fulfillment of the requirements for the degree of Master of Science.

_____

Millie M. Georgiadis, Ph.D., Committee Chair

Master's Thesis
Committee

_____

William F. Bosron, Ph.D.

_____

Frank A.Witzmann, Ph.D.

ACKNOWLEDGMENTS

I would like to extend my gratitude to those who made this thesis possible. My experience would not have been possible without the help of mentors, friends and family who supported me along the way. Firstly, I am grateful for being given the opportunity to work and study under the guidance of Dr. Millie Georgiadis. She has taught me to think critically about my experiments and guided me through the process. Her advice, criticism, and encouragement as enabled me to complete this work, and the training I have received will follow me throughout my career.

I would also like to thank Millie's lab as a whole for giving me the training and support necessary. Millie's lab has included many very intelligent and delightful people with diverse backgrounds, all who contributed to my training. I would specifically like to thank Sherwin Montano, Debanu Das, and Ian Fingerman who helped me from the very early days and sparked my initial interest in research. Thanks also to Hongzhen He and LaTeca Glass who have become good friends and mentors, and to Jen Earley, my go-to source for all problems. And a very special thanks to my favorite lab mate and best friend, Kristie Goodwin, who inspired me both in and outside of lab. I will always be grateful for her friendship.

I thank my committee members, Dr. Bill Bosron and Dr. Frank Witzmann, for taking time out of their schedules to meet with me. I appreciate their insights into my project.

Thanks also to our collaborators Dr. Michael Gross and Dr. Dian Su from Washington University in St. Louis who made this research possible.

And finally, thank you to my dear husband, Brad, and my beautiful daughter, Alma.

ABSTRACT

Sarah Ann Delaplane

MASS SPECTROMETRIC APPROACHES
TO PROBING THE REDOX FUNCTION
OF APE1

Human apurinic/apyrimidinic endonuclease 1 (hApe1) is a multi-functional protein having two major functions: apurinic/apyrimidinic endonuclease activity for DNA damage repair and redox activity for gene regulation. Many studies have shown the action of Ape1 in the base excision repair pathway leading to cell survival. It has also been reported that Ape1 reduces a number of important transcription factors that are involved in cancer promotion and progression. Though the repair activity is well understood, the redox mechanism is not yet clear.

What is known about Ape1 is its structure and that it contains seven cysteines (C65, C93, C99, C138, C208, C296, and C310), none of which are disulfide bonded. Two of these cysteines, C99 and C138, are solvent-accessible, and C65, C93, and C99 are located in the redox domain. It is believed that one or more cysteines are involved in the redox function and is hypothesized that hApe1 reduces the down-stream transcription factors by a disulfide exchange mechanism.

E3330, (2E)-3-[5-(2,3-dimethoxy-6-methyl-1,4-benzoquninoyl)]2-nonyl-2-propenoic acid, is a specific inhibitor for the redox function of hApe1. The interaction mechanism is not known. Using N-Ethylmaleimide (NEM) chemical footprinting,

combined with Hydrogen/Deuterium Exchange (HDX) data, we propose that a locally unfolded form coexists with the folded form in an equilibrium that is driven by irreversible NEM labeling, and that E3330 interacts with and stabilizes this locally unfolded form. This locally unfolded form is thereby proposed to be the redox-active form. We further support this claim with LC-MS/MS analysis showing an increase of disulfide bonds induced by E3330 among the cysteines in the redox domain, which would be too far apart from each other in the folded form to form a disulfide bond.

We also studied three analogs of E3330. The need for an E3330 analog is to develop a more efficient and effective compound that would allow for sub-micromolar levels of activity (E3330 requires a micromolar amount). Study of the analogs will also allow us to gain perspective of the mechanism or mechanisms of E3330's activity in Ape1's redox function.

Millie M. Georgiadis, Ph.D., Committee Chair

TABLE OF CONTENTS

List of Tables viii

List of Figures ix

Chapter I Overview of Ape 1

- Introduction of Ape1 Function 1
- Ape1 in the Base Excision Repair Pathway 2
- Ape1's Redox Function 3
- Exposing Redox Function Through Structure 4
- Ape1's Role as a Cancer Therapeutic 6

Chapter II E3330 Studies 9

- Interaction of E3330 with Ape1 9
- Material and Methods 11
- Results 15
- Discussion 19

Chapter III E3330 Analog Studies 23

- Introduction to the E3330 Analogs 23
- Materials and Methods 25
- Results 28
- Discussion 30

Chapter IV Conclusion 31

Figures 34

References 51

Curriculum vitae

LIST OF TABLES

1. Hydrogen/Deuterium Exchange Results.....20

2. Disulfide Bonds Formed.....21

LIST OF FIGURES

1. BER pathway 34
2. Ape1's role in BER pathway 35
3. Ape1's role in redox of transcription factors 36
4. X-ray crystal structure of Ape1 37
5. Chemical Structures of E3330 and NEM 38
6. ESI mass spectra wtΔ40Ape1 and mutants with NEM labeling 39
7. Kinetics of wtΔ40Ape1 with E3330 and NEM 40
8. ESI mass spectra of wtΔ40Ape1 with E3330 and NEM 41
9. ESI mass spectra of wtΔ40Ape1 at 30 min and 4 hr 42
10. ESI mass spectra of denatured FLApe with NEM 43
11. Scheme of Ape1 unfolding 44
12. ESI mass spectra wtΔ40Ape1 increased temperature 45
13. ESI mass spectra of hΔ40Ape1 mutants 46
14. Chemical structure of E3330 analogs: RN7-60b, RN10-52, RN8-51 47
15. ESI mass spectra of FLApe1 and all E3330 compounds 48
16. ESI mass spectra of FLApe1 and analogs showing modification 49
17. Mechanism of covalent vs. reversible inhibition of Ape1 redox 50

CHAPTER I

Overview of Ape

Introduction of Ape1 Function

Human apurinic/apyrimidinic endonuclease 1 (hApe1) is a multi-functional protein having two major functions: apurinic/apyrimidinic endonuclease activity for DNA damage repair and redox activity for gene regulation (*1*). Not only is Ape1 involved in vital functions, its importance to the cell is that there is no backup for its responsibilities. This is demonstrated by the fact that it has not been possible to generate an animal knockout model. Ape1 mouse knockouts are embryonic lethal, and no viable cell lines have been established that are completely deficient for Ape1 (*2*).

It had been reported that Ape1's redox and repair domains were separate: redox within the N-terminal and repair within the C-terminal regions (*3*). However, these functional domains do not coincide with the structural domains of the protein. A recent review of Ape1 (*1*) discusses the structural similarities in regard to topology and endonuclease activity sites between hApe1 and *E. coli* exonuclease III (the AP endonuclease found within *E. coli*); however, redox function is only found in mammals. Human Ape1 does have an additional 62 N-terminal residues, but these alone cannot be responsible for redox activity considering that zebrafish also has the additional N-terminal residues and no redox activity. What is needed for hApe1 redox function remains a question worth investigating.

Ape1 in the Base Excision Repair Pathway

DNA damage can occur from of variety of sources, including alkylation, deamination, and oxidation of bases. Base Excision Repair (BER) is the pathway used for repairing this DNA damage (*4-6*). Alkylation of bases is caused by exposure to either endogenous or exogenous agents. Another source, deamination of cytidines and adenines, occurs spontaneously. DNA damage can also be due to reactive oxygen species in normal cellular processes or environmental or chemotherapeutic agents. BER is needed for repairing DNA damage caused by these sources, and Ape1 plays a key, irreplaceable role in it. Ape1 is needed in the second step of the base excision repair (BER) pathway to cleave the phosphodiester bond 5' of an abasic site (or AP site) (Figure 1). Abasic sites are generated by DNA glycosylases, which excise a base damaged by alkylation or oxidation, and then subsequently processed by Ape1, leaving a 3'-OH and 5'-deoxyribose phosphate (*7-9*). DNA glycosylases, both monofunctional and bifunctional, initiate BER by recognizing oxidized or alkylated bases. The monofunctional form excises the damaged base creating an abasic site, which is the site that Ape1 acts upon. Bifunctional glycosylases excise the damaged base and nick the phosphodiester backbone 3' to the AP site. Ape1 then hydrolyzes the phosphodiester backbone 5' to the AP site creating 3' OH and 5' deoxyribose phosphate (5' dRP) ends (*10, 11*) (Figure 2), which are processed by subsequent enzymes of the BER pathway. Without the removal of a damaged base resulting in an AP site, there could be a block to DNA replication and genetic instability (*12*). Ape1 is responsible for 95% of the endonuclease activity in the cell (*7, 8*), and there is no replacement for its function. Therefore, Ape1 is vital for survival. Ape1 is also

responsible for recruiting other DNA repair proteins for BER through protein-protein interactions and indirect interactions (*1*).

Ape1's Redox Function

The search for Ape1's redox function begins with an attempt to identify the nuclear factor responsible for reducing transcription factor Activator protein-1 (AP-1). Fos and Jun were shown to form a heterodimeric complex that binds to transcriptional control elements containing AP-1 binding sites that regulate gene expression (*13*). Cell growth and differentiation are controlled through the regulation of gene expression by extracellular signals.

In early experiments, as well as the ones we are currently employing, cysteine residues were being monitored. Cysteine residues are often required for functional and structural properties of proteins and can be used to define characteristic protein domains. Usually cysteine residues are conserved across phylogenetic boundaries and among gene families (*14*). It was shown that reduction of a conserved cysteine residue in the DNA-binding domains of Fos and Jun by chemical reducing agents or by a nuclear redox factor stimulates DNA-binding activity. Ape1 was first identified and characterized as this nuclear factor, termed as a redox effector factor-1 (Ref-1) (*15, 16*). Ref-1 stimulates AP-1 DNA-binding activity in Fos and Jun through a mechanism involving the conserved Cys residues. It did not alter the DNA-binding specificity of Fos and Jun, which begun an examination of a novel redox component of the signal transduction processes that regulates eukaryotic gene expression.

These studies led to the identification of a redox mechanism that is required to modulate AP-1 DNA binding activity *in vitro* (*15, 17*). Redox regulation was mediated by a conserved cysteine residue located in the DNA-binding domains of Fos and Jun that was flanked by basic amino acids (*17*). Fos and Jun could be converted to an inactive state by chemical oxidation or modification of this residue (*18*). At that time, there was a lot of debate on the role of redox switching in regulating transcription factor function because of the generally accepted view that the intracellular environment is reducing and very little was known about the redox environment of the nucleus.

After the discovery of Ref1's involvement in reducing AP-1, the enzyme was later identified as Ape1 (*14*). Since the initial discovery of reducing AP-1, Ape1 has been reported to reduce a number of other important transcription factors including NFκB, p53, PAX, and others (*19-25*) (Figure 3). The redox activity of Ape1 plays an important role in regulating the expression of a large number of DNA repair proteins. The mechanism of hApe1 in the reduction of transcription factors is unclear.

Exposing Redox Function Through Structure

Human Ape1 contains seven cysteines (C65, C93, C99, C138, C208, C296, and C310). Two of these (C99 and C138) are solvent-accessible, as shown in the crystal structure (Figure 4) (*26-29*). Three cysteines, C65, C93, C208, are buried in Ape1's core. Not only does the structure show no disulfide bonds, there are no cysteines within range to allow for a disulfide bond. Cysteine 93 and C208 are the two cysteines that reside closest to one another, but their sulfur atoms remain 3.5 Å apart (typically a disulfide bond is no longer than 2.2 Å).

Investigating Cys residues within Ape1 was based on the finding that a cysteine residue within the DNA-binding domain of the transcription factor c-Jun was subject to oxidation leading to loss of DNA-binding and was reduced by Ape1 (*14, 17, 30*). Because Ape's redox activity is unique to the mammalian form (unlike endonuclease activity which is also seen in all organisms, including bacteria), C65 became a focus because it is also unique to mammals (*29*).

In a study employing both site-directed mutagenesis and *in vitro* electrophoretic-mobility-shift-assay (EMSA) analysis, the role of cysteine residues in Ape1's redox activity has been previously investigated by mutating each of the cysteines to an alanine. Of Ape1's seven cysteines, only C65A was found to be redox inactive (*31*).

Only one publication (*32*) reported that C65 was not an essential residue. This study reported a viable C64A (64 in mouse is equivalent to 65 in human) knock-in mouse, which challenged the importance of this residue for cell survival. This finding was counter challenged by another study that examined the role of Cys65 in the redox activity of Ape1 using zebrafish, which is 65% identical to human Ape1. In looking at the structures, the zebrafish structure is similar to human Ape1 with five of the seven cysteines found in mammalian Ape1 being conserved (*29*). The two that are not conserved are Cys65 and Cys138. Analysis of the Cys residues within vertebrates suggests that the presence of Cys65 is unique to mammals and distinguishes their Ape1 from that in nonmammalian vertebrates (*29*). The zebrafish Ape (zfApe) contains the catalytic residues for its endonuclease activity but instead of including a cysteine at the 65 position, it has Thr58. A T58C zfApe mutant was made and tested for redox activity

along with a native zfApe sample. The native zfApe was inactive for redox activity; however, the mutant T58C zfApe was as active as the human Ape1 (*29*).

This evidence shows the importance of the Cys65 in the redox activity of Ape1. How this cysteine is made accessible to the transcription factors is unknown. Again, the crystal structures show that Cys65 is buried within the protein and not accessible to any transcriptional factors, implying that Ape1 would have to undergo a conformational change.

Ape1's Role as a Cancer Therapeutic

It is recognized that DNA-damaging agents are useful in killing cancer cells (*33*). The up regulation or activation of a number of different pathways that cause resistance of the cancer cells to the treatment with DNA damaging agents is a problem. Pathways included are those involved in signaling, multidrug resistance, cell-cycle checkpoints, antiangiogenesis, and others as potential approaches to treat and kill cancer. There has been a focus on blocking the ability of a cancer cell to recognize and repair the damaged DNA that results from front-line cancer treatments, chemotherapy, and radiation. One of these systems includes DNA-repair enzymes, such as Ape1, leading to resistance and failure of the agent to kill the cancer cells (*6, 34*). One possible strategy for preventing resistance and improving efficacy of the DNA-targeting agents would be to inhibit the DNA-repair enzyme responsible for resistance.

Another approach, that has not been extensively studied, is targeting the redox function of Ape1 to prevent cell proliferation. Intracellular redox has been suggested as a regulator of growth in cancer cells (*35*). Ape1 is overexpressed in numerous cancers,

including prostate and bladder cancers (*36, 37*). In these and other studies, Ape1 overexpression is associated with an adverse prognosis (*36*) and/or resistance to radiation and chemotherapeutic agents (*38*).

Regulation of the intracellular redox environment is critical for cell viability and maintenance of cellular homeostasis. An Ape1 deficient cell line cannot be generated because Ape1 is essential for early embryonic development in mice (*39*). Therefore identification and development of a specific inhibitor of this protein will significantly help as a tool in Ape1 functional study and therapeutic potential.

Both of Ape1's functions (endonuclease and redox) can be used in developing inhibitors as potential cancer therapeutics. We focused on blocking the redox function of Ape1. These studies are divided into two parts. The first is development of a recent novel approach to cancer therapeutic agents targeting the redox activity of hApe1 (*1*, *40*). A quinone derivative E3330, (2E)-3-[5-(2,3-dimethoxy-6-methyl-1,4-benzoquninoyl)]2-nonyl-2-propenoic acid, was found to inhibit specifically the redox ability of hApe1 (*41-44*). E3330 is able to kill a variety of cancer cells but does not significantly affect normal cells (*1*). Using this inhibitor, we conducted a series of experiments to elucidate the Ape1 redox mechanism (*45*).

The second chapter includes a characterization of analog compounds of E3330: RN7-60, RN8-51, and RN10-52. These compounds were studied in a recent publication (*46*), and further investigation is required to determine their value as redox inhibitors. The need for an E3330 analog is to develop a more efficient and effective compound that would allow for sub-micromolar levels of activity (E3330 requires a micromolar

amount), and to gain perspective of the mechanism or mechanisms of E3330's activity in Ape1's redox function.

CHAPTER II

E3330 Studies

Interaction of E3330 with Ape1

E3330 (Figure 5), a quinone derivative, is otherwise known as 2E)-3-[5-(2,3-dimethoxy-6-methyl-1,4-benzoquninoyl)]2-nonyl-2-propenoic acid. It was found to inhibit specifically the redox ability of hApe1 without affecting its endonuclease activity (*42-44*, *47*). E3330 is able to kill a variety of cancer (i.e., ovarian, colon, lung, breast, brain, pancreatic, prostate, multiple myeloma) cells but does not significantly affect normal cells (*41*). No studies have successfully shown the mechanism by which E3330 inhibits Ape1's redox activity. There's yet to be confirmation of the location of the binding site and the conformational changes, if any, associated with hApe1 binding to E3330.

Earlier studies separated Ape1 from Jurkat cell extract on beads tagged with E3330, making Ape1 the primary target of E3330 (*41*). Using surface Plasmon resonance (SPR), it was reported that the binding constant for hApe1 and E3330 is 1.6 nM, which indicates strong and specific binding between hApe1 and E3330. Further studies showed E3330's ability to block Ape1 from reducing NFκB, prohibiting redox activity (*48*).

Previous studies of E3330 show an inhibition of Ape1's redox activity (*44*). Furthermore, it was demonstrated that the humanized zebrafish Ape1, previously demonstrated to gain redox activity (*29*), was also inhibited by E3330 (*44*). This study also showed that the inhibition of the redox activity of Ape1 had no effect on Ape's repair function.

E3330 was also able to block the redox function of Ape1 in two ovarian cancer cell lines by using a transactivation reporter assay in a dose-dependent manner (*44*). This data shows the role of Ape1 in redox activation of downstream targets, and it demonstrates that E3330 is a small molecule that blocks transcription-factor activation. Of particular interest are the transcription factors that are involved in cancer cell growth and proliferation, such as NFκB and AP-1.

Other studies demonstrated that blocking the redox function of Ape1 led to blocking cell proliferation (*42*). The benefit of using E3330 to approach the redox function of Ape1 is that it doesn't use the overexpression of Ape1, Ape1 antisense oligonucleotides, or Ape1 siRNA, as reported in studies had that showed altering Ape1 levels leads to blockage of cell growth and increased cancer cell sensitivity (*6, 38, 49-57*). The approaches from those studies caused a change in the total cellular content level of Ape1 and, in the case of antisense or siRNA, removed all of the Ape1 functions, not just the repair or redox activities. Because Ape1 has multiple functions as well as protein–protein interactions with other DNA repair and signaling proteins, the increase or decrease of Ape1 protein may result in inaccurate findings. Use of specific small-molecule inhibitors of Ape1 redox activity, like E3330, focuses on the exact role of native levels of Ape1 in various cancer, disease, and normal cellular functions.

To help understand the redox activity of Ape1 with important transcription factors, the inhibitory activity of E3330 was examined. A crystal structure of an Ape1/E3330 complex has yet to be solved, and so a different approach was pursued in this study.

In an effort to detail further the redox mechanism, we developed a chemical footprinting/mass spectrometric assay using *N*-ethylmaleimide (NEM) (Figure 5), an irreversible cysteine modifier, to characterize the interaction of the redox inhibitor, E3330, with Ape1. NEM is a water-soluble, small molecule that specifically reacts with solvent-accessible cysteines via a Michael addition. This modification is irreversible. This reagent is widely used in protein footprinting (*58-61*). Our results show an interaction between E3330 and Ape1 and provide new information on the redox mechanism of Ape1.

Material and Methods

Compound

E3330 was synthesized as previously described (*44*).

Expression and purification of proteins

wtΔ40APE1

A truncated Ape, hΔ40Ape1 (40-318), was cloned into pet28a vector using BamH1 and XhoI restriction sites with an N-terminal hexa-His affinity tag , then transformed into Rosetta (DE3) *E. coli* (Novagen). The cells were grown in 6 L of LB media with 100 µg/mL kanamycin and 34 µg/mL chloramphenicol until the OD at 600 nm reached 0.5, and then induced for 4 hours with 1 mM IPTG at 37ºC. The cultures were harvested by centrifugation at 4000 × *g* for 30 minutes, and the pellets were stored at -80ºC. The cell pellets were each resuspended in 20 mL of 50 mM sodium phosphate buffer pH 7.8, 0.3 M NaCl, 10 mM imidazole, and then lysed by using a French press

(SLM-AMINCO, Spectronic Instruments, Rochester, NY) at 1000 psi. The suspension was centrifuged at 35,000 rpm for 35 min, and the supernatant was then loaded on a Ni-NTA column at 4ºC. The protein was eluted with a linear imidazole gradient (0.02– 0.5 M), and fractions containing hΔ40Ape1 were further purified on an S-Sepharose column using 50 mM MES pH 6.5, 1 mM DTT, and a linear NaCl gradient (0.05–1 M). The fractions were incubated overnight with 2 units/mg of thrombin to cleave the N-terminal hexa-His tag and then subjected to a final S-Sepharose chromatographic purification step. Fractions containing hΔ40Ape1 were then concentrated using Amicon Ultra centrifugal concentrators (Millipore, Billerica, MA) and stored at -80ºC. Site-directed mutagenesis using the Stratagene Quikchange kit (La Jolla, CA) was used to introduce C99A, C138A, and C99A/C138A substitutions in hΔ40Ape1.

Primers for mutation:

C99A 5'—CAAGAGACCAAA **GCC** TCAGAGAACAAACTACCAGC—3'

3'—GTTCTCTGGTTT **CGG** AGTCTCTTGTTTGATGGTCG—3'

C138A 5'—GGCCTGCTTTCCCGCCAG **GCC** CCACTCAAAGTTTCTTACGGC—3'

3'—CCGGACGAAAGGGCGGTC **CGG** GGTGAGTTTCAAAGAATGCCG-3'

Substituted hΔ40Ape1 proteins were expressed and purified as described for wtΔ40Ape1 and confirmed by DNA sequencing analysis.

Mass Spectrometric Analysis

NanoESI (nESI) MS

Δ40Ape1 was incubated in 1 M ammonium acetate (pH 7.5) with or without E3330 at room temperature (RT) for 4 h. Protein samples were analyzed by nESI-MS in

the positive-ion mode on a Bruker MaXis UHR-TOF (ultra-high resolution time-of-flight) (Bruker Daltonics Inc., Fremont, CA) at a flow rate of 25 nL/min. The capillary voltage was set at -(1000-1200 V). Dry gas and temperature were at 5.0 L/min and 50ºC, respectively. The instrument was externally calibrated by using "Tuning Mix" (Agilent Technologies, Santa Clara, CA). The spray tips were made in-house by pulling a 150 µm i.d. × 365 µm o.d. fused silica capillary with a P-2000 Laser Puller (Sutter Instrument Co., Novato, CA). A four-step program was used with the parameter setup as follows with all other values set to zero: Heat = 290, velocity = 40, delay = 200; Heat = 280, velocity = 30, delay = 200; Heat = 270, velocity = 25, delay = 200; Heat = 260, velocity = 20, delay = 200. Tips were cut accordingly to allow a good spray under the experimental conditions. For each sample, a new tip was used to avoid cross contamination.

NEM Chemical Footprinting and ESI-MS

For NEM labeling, 10-20 µL of Δ40Ape1/NEM (Δ40Ape1:NEM = 1:5, mol/mol) and Δ40Ape1/NEM/E3330 (Δ40Ape1:NEM:E3330 = 1:5:5, mol/mol/mol) Δ40Ape1 samples were incubated in 10 mM HEPES buffer (pH 7.5) at room temperature; the protein concentration was 100 µM. At a certain time, a 1 µL aliquot was removed and quenched with 1 µL of 20 mM DTT. Mass spectra were collected on the Bruker MaXis UHR-TOF or Waters Micromass Q-TOF instrument (Waters Micromass, Manchester, UK). The parameters for MaXis mass spectrometer are as follows: Capillary voltage was set at -3600 V. Nebulizer pressure was 0.4 bar, and dry gas was at 1.0 L/min. The drying temperature was 180ºC. The instrument was calibrated using Tuning Mix (Agilent Technologies, Santa Clara, CA) as the external mass calibrant. The parameters for the

Waters Q-TOF instrument are listed below: The Z-Spray source was operated at 2.8 kV, the cone voltage was 150 V, and RF lens was 50. The source temperature and desolvation temperatures were 80ºC and 180ºC, respectively. The collision energy was 10 eV, and the MCP detector was 2,200 V. Protein samples were loaded on an Opti-Guard C18 column (10 mm × 1 mm i.d., Cobert Associates, St. Louis, MO) for desalting and then eluted to mass spectrometer using 50% (v/v) acetonitrile with 0.1% formic acid (FA) at 10 μL/min. Spectral deconvolution was performed using MaxEnt.

Data Processing of NEM-Labeling (performed by Don Rempel, Washington University)

A number of the equation parameters were extracted from the kinetic data by nonlinear least squares fitting of theoretical signals, computed from the parameter dependent system state trajectories, to experimental data. The system state was a vector that has the solution chemical species concentrations as the vector coordinates. In each trial of the search, the postulated parameters together with the system state of concentrations permitted the calculation of the time rate of change of the state by computing the fluxes into and out of each species as described by the system equations. This process implemented a vector first-order ordinary differential equation, which was solved by numerical integration for the time interval of reaction initiation to the longest reaction time to give the state time trajectory in each fitting trial. For comparison with the experiment data, the theoretical signal for each Ape1 species was computed as a fraction of all Ape1 species concentrations that were first weighted by a relative sensitivity factor that varied linearly with slope g_N with the number of NEMs attached starting with one for

Δ40Ape1 by itself. The calculations were carried out in the computer application Mathcad 14.0 M010 (Parametric Technology Corporation, Needham, MA). The numerical integration of the differential equation was carried out by the adaptive fourth-order Runge-Kutta function "Rkadapt".

Denatured Ape1 and ESI MS

A sample of 10 μM FLApe was denatured by 2 M guandinium hydrochloride and incubated along with 70 μM NEM in 10 mM Tris pH 7.5 buffer. The guanidium hydrochloride was gradually dialyzed out in two steps reducing the concentration by 1 M in each step. This sample and an untreated native full-length Ape1 were then subjected to ESI analysis using an Agilent 6520 Q-TOF instrument. Deconvolution was done using Mass Hunter software that is part of that system.

Results

Initially, wtΔ40Ape1 and the 3 mutants (C99A, C138A, and C99A/C138A) were incubated with NEM and without E3330 to verify the labeling that would occur for Ape1 untreated with E3330. wtΔ40Ape1 results in the formation of a +2 NEM modified species as indicated by a shift in mass of 250 Da (Figure 6A). The C99A and C138A show a reduction from +2 NEM for wtΔ40Ape1 to +1 NEM (Figure 6B and C), and for the double mutant there is no longer any NEM bound (Figure 6D). These products form within 30 s of the addition of NEM.

A time course was done with wt that shows nearly 100% modification of wtΔ40Ape1 within 10 minutes at room temperature (Figure 7A). The time course shows

the gradual disappearance of the peaks corresponding to unmodified cysteines in the mass spectrum. Of the seven Cys residues within Ape1, only Cys 99 and Cys 138, the two solvent-accessible Cys residues, are labeled at room temperature. The C99A mutant and C138A mutant both show a reduction from +2 NEM for wtΔ40Ape1 to +1 NEM, and for the double mutant there is no longer any NEM bound. The sites of modification were verified by LC-MS/MS.

When Δ40Ape1 was incubated with both NEM and E3330, the +2 NEM product again forms quickly. However, over time, a second major product corresponding to the addition of 7 NEMs was observed (Figure 7B). This peak is only seen in the presence of E3330. Trypsin digestion coupled with LC-MS/MS analysis conclusively indicates that the protein is modified on the five remaining cysteines, which were originally solvent-inaccessible, and not on other reactive amino-acid residues.

After a 6 h incubation of Δ40Ape1 with NEM , with and without E3330, a small amount of + 3 NEM product was observed (Figure 8); LC-MS/MS analysis indicates that this product comes from the NEM reaction with other, non-Cys, solvent-accessible sites (e.g., K, H, and the $–NH_2$ at the terminus).

To test whether the results of the Δ40Ape1/E3330/NEM experiment were caused by the DMSO, in which E3330 was dissolved, reactions of Δ40Ape1/NEM alone, with E3330, and with DMSO were incubated at 30 minutes and 4 hours and then analyzed by global ESI-MS (Figure 9). At 30 min, all three samples appeared identical with a +2 NEM. At 4 hours, all samples still have the same +2 NEM peak; however, they also have a small +3 NEM peak. The E3330 sample also includes a +7 NEM peak.

To prove that E3330 did not just denature the protein, forming the +7 product, a sample of Ape1 with E3330 was incubated for 24 hr at room temp, followed with NEM at room temp for 0.5 hr. Only the +2 NEM product was observed, without any +7 NEM product. If E3330 were denaturing Δ40Ape1, we would have expected to modify all 7 Cys residues with NEM.

Also, to verify that there wouldn't be NEM labeling higher than +7 NEM showing nonspecific binding, we did a denaturing experiment in which a sample of 10 μM FLApe was denatured by 2 M GuHCL and treated with 70 μM NEM. For the untreated native FLApe sample (Figure 10A), the only major peak is the parent peak for full-length Ape1 labeled P with an observed mass of 35,641.3 (expected 35,641.5). The denatured NEM treated FLApe sample (Figure 10B) resulted in 4 major peaks including the parent peak labeled P, along with +5 (36,266.6), +6 (36,392.4), and +7 (36,517.3) NEM modifications to the parent molecule. No higher mass peaks for modification with NEM beyond +7 NEM were observed.

Other than the slight presence of the +3 peak, there are no intermediates between +2 and +7 NEM. To see a gradual unfolding of Ape1, I took time points every 30 min for 4 hrs of a sample of Ape1/E3330/NEM. At 30 min only the +2 NEM product was detected. But there is no gradual labeling of Cys residues. Around 3 hours, both +3 and +7 were detected. Over the same time period and temperature, no +7 NEM modified species formed in the reaction of Δ40Ape1 with NEM in the absence of E3330.

However, what could be seen was the +2 NEM species decreasing over time while the +7 NEM product was increasing (Figure 7). The lack of intermediates even with a 5 molar excess of NEM suggest that there is a rapid conversion from the +2 to +7

NEM state once one or more of the five Cys residues remaining in the +2 NEM modified Δ40Ape1 reacts with another NEM. Analysis performed by LC-MS/MS confirmed that all seven Cys residues in the +7 NEM species were modified. As for the small amount of the +3 NEM species, there is no significant change in its quantity throughout the reaction. This leads us to the conclusion that it is not an intermediate that leads to the formation of the +7 NEM product. There is also an equal amount of this product observed without the addition of E3330.

Based on these results, it is proposed that a rate-limiting step occurs after the rapid formation of the +2 NEM species, in which Ape1 undergoes a conformational change from fully folded to locally unfolded state (Figure 11). It is within this state that E3330 binds to and stabilizes Ape1, allowing the Cys residues to be exposed and then bound with NEM, so that we are able to observe the +7 NEM species.

Up to this point, all samples had been incubated at room temperature. If the temperature was raised to 37ºC, we would expect to see the reaction time required to form the +7 NEM modified Δ40Ape1 decrease, and for this unfolded state to be observed without the addition of E3330. As shown in Figure 12A, Δ40Ape1 treated with NEM at 37ºC without E3330 will form a small percentage of +7 NEM, supporting that the protein does undergo this conformation change. For the sample treated with E3330 (Figure 12B), the time for the +7 NEM product to appear decreased from 3 hours to 30 minutes. This decrease in time shows that Ape1 adopts the locally unfolded state, thus establishing an equilibrium for the 2 conformations.

It was of interest to determine whether or not any specific cysteines were required in order for Ape1 to undergo this conformational change. Because of the importance of

C65 in Ape1 redox function, is it required for Ape1 to adopt an alternate conformation? Or is the modification of the 2 solvent accessible cysteines, 99 and 138, required for the remaining cysteines to be labeled? The following mutants were made for Δ40Ape1: C65A, C99A, C138A, C99A/C138A. They were incubated with NEM and E3330 then analyzed by global ms. All mutants were observed to undergo a conformational change that allowed for the remaining cysteines to be modified (Figure 13). This result indicates that labeling of the buried Cys residues in Δ40Ape1 does not depend on the presence of Cys 65, Cys 99, or Cys 138.

Discussion

Additional Studies

To further test our hypothesis that E3330 interacts with a locally unfolded form of hApe1, maintaining it in a more opened form, and that this leads to the Δ40Ape1+7 NEM adduct, we relied on our collaborators to perform hydrogen/deuterium exchange (HDX) experiments to analyze the exchange of amide protons with deuterium in different adducts of Ape1. If our hypothesis is correct, then we should be able to see differences in the extent of HDX for the Δ40Ape1+7 NEM adduct in comparison with the Δ40Ape1+2 NEM adduct. Furthermore, if the Δ40Ape1+3 NEM adduct is a "dead end" as we proposed, its extent of HDX should match that of the Δ40Ape1+2 NEM adduct.

As reported (*45*) the +2 NEM adduct exchanges 144 amide hydrogens whereas for the Δ40Ape1+7 NEM adduct, the corresponding number of exchanges is 188. With a kinetic model reported earlier (*62*), the data was fitted and the exchanging amides were categorized into the number of fast, intermediate, and slow.

Based on the model, we were able to assign the number of amide protons of each type. The results:

Table 1 Hydrogen/Deuterium Exchange Results

	Fast	Intermediate	Slow
ApeΔ40	78 ± 2	25 ± 4	43 ± 1
ApeΔ40 + 2 NEM	81± 1	20 ± 4	43 ± 2
Ape Δ40 + 3 NEM	81 ± 2	19 ± 2	41 ± 1
Ape Δ40 + 7 NEM	136 ± 3	14 ± 1	38 ± 4

The number of fast exchanging adducts has increased substantially for the unfolded conformation as a result of the reaction with NEM. Δ40Ape1+7 NEM has 40 more exchanging amide H's than Δ40Ape1/ Δ40Ape1+2 NEM/ Δ40Ape1+3 NEM, which supports the existence of a locally unfolded form. Considering that there are 278 total amide hydrogens in the protein, we see that only 68% underwent exchange even for the protein modified with seven NEMs, indicating that Δ40Ape1+7 NEM form is a partially unfolded form and not a completely denatured one. The HDX results for Δ40Ape1, Δ40Ape1+2 NEM and Δ40Ape1+3 NEM proteins are similar, confirming that these three species have the same conformation, and that additions of NEM to the solvent accessible Cys residues and to other reactive sidechains do not change the conformation of Δ40Ape1.

Our collaborators also performed LC-MS/MS to examine disulfide bond formation (*45*). Considering the requirement of Cys65 for redox, the Cys65 would serve as the nucleophilic thiol in the reduction of transcription factors by Ape1. For this thiol-

mediated disulfide exchange reaction to occur, it must exist in a reduced state. This would be monitored by looking at disulfide bonds and the effect of E3330 on their formation. LC-MS/MS analysis of tryptic peptides showed an increase of disulfide bonds when treated with E3330. Table 2 shows the percent of disulfide bonds for the bonds listed:

Table 2 Disulfide Bonds Formed

	% No E3330	%With E3330
C65-C93	0.16	8.2
C93-C99	0.04	5.8
C93-C138	0.01	2.6
C65-C99	0.01	2.6

Both Cys65 and Cys93 play an important role in the redox activity of Ape1(*29, 31*), and so formation of disulfide bonds C65-C93, C65-C99, and C93-C99 would be expected to impact the redox activity of Ape1.

Combining the Data

With all data considered, we can conclusively say that Ape1 requires a conformational change in order to obtain the +7 NEM adduct. When incubated with E3330 or placed under elevated temperature conditions, the locally unfolded form of the +2 NEM state of Ape1 is sufficiently long-lived that it can be captured by reaction with NEM to give a +7 NEM modified Ape1. In the reaction for the +2 NEM state, the NEM

bond is irreversible (Figure 11), and the slow step of the reaction is the local unfolding of the +2 NEM modified Ape1. E3330 does not create this unfolding, but drives the equilibrium toward the unfolded form. It's in this unfolded state of Ape1 that some previously buried Cys residues are accessible and able to react with NEM producing the +7 NEM species. By chemical footprinting with NEM in the presence and absence of E3330, we see evidence for a locally unfolded state of Ape1 through these newly exposed and labeled cysteines.

This chemical footprinting combined with the HDX kinetics gives strong evidence for the existence of a partially or locally unfolded conformation of Ape1. The HDX experiments, as determined by mass spectrometry, show an increase of approximately 40 deuterium atoms in the +7 NEM adduct when compared to both the native Ape1 and +2NEM adduct. The unfolding in our experiments helps us to explain the exposure for the buried residue Cys65, which was previously shown to be a necessity for redox function.

In our search for understanding the mechanism by which E3330 inhibits the redox activity of Ape1, we propose that E3330 interacts with the locally unfolded state of Ape1, stabilizing it so that the normally buried Cys residues can react with NEM. In shifting the equilibrium toward the locally unfolded state of Ape1, E3330 also increases disulfide bond formation in Ape1. This increase could be due to a stabilization of the unfolded conformation by E3330 or due to a reversible modification of Cys residues, making them susceptible to nucleophilic attack by a sylfhydryl and thereby resulting in disulfide bond formation.

CHAPTER III

E3330 Analog Studies

Introduction to the E3330 analogues

It's been shown in previous studies that E3330 binds specifically to Ape1. E3330 blocks Ape1's redox function with transcription factors by not allowing them to be converted from an oxidized to a reduced state, therefore preventing them from binding to their target DNA (*44, 46*). Also, E3330 blocks angiogenesis in *in vitro* and *in vivo* models (*43, 44, 63*).

The need for an E3330 analog is to develop a more efficient and effective compound that would allow for sub-micromolar levels of activity (E3330 requires a micromolar amount), and to gain perspective on the mechanism or mechanisms of E3330's inhibition of Ape1's redox function.

Results of synthesis of E3330 analogs (Figure 14) were recently published (*46*), and further investigation was performed on the 3 most promising ones: RN8-51, RN10-52, and RN7-60 (*64*). Using EMSA (electrophoretic mobility shift assay) (*44*) with AP-1 as the transcription factor target, these analogs blocked the redox function of Ape1. Also, their IC50's were at least ten times lower than E3330. E3330 had an IC50 of 20 μM where as RN8-51, RN10-52, and RN7-60 were 0.5, 0.75, and 1.5 μM respectively (*64*).

From a recent publication (*64*), studies were performed in order to examine the specificity of the compounds with Ape1. The EMSA studies were repeated substituting thioredoxin, a cellular redox protein, for Ape1. Thioredoxin has been shown to reduce AP-1 *in vitro*. These studies concluded that increasing the amounts of E3330, RN8-51,

and RN10-52 decreased the binding of AP-1 to DNA by blocking the ability of Ape1 to reduce AP-1, but did not similarly inhibit reduction by thioredoxin. RN7-60 affected both Ape and thioredoxin. Though it affects Ape1 at greater levels, it is not an Ape1-specific redox inhibitor. As for E3330, RN10-52, and RN8-51, they only affect Ape1, and therefore are Ape1-specific redox inhibitors.

This study also proved that the analogs are specific to Ape1's redox function and do not affect it's DNA repair function, as also seen with E3330 previously (*44, 65*). None of the analogs blocked Ape1 repair endonuclease activity, supporting that they are specific to redox function.

Cell-based transactivation assays were performed to test whether the redox function would be blocked in cells with analogs as it was for E3330 (*1*). Using SKOV-3x, an ovarian cell line, NF-κB binding sequence upstream of a luciferase reporter was expressed. NF-κB was dose-dependently unable to bind with an increasing amount of E3330 and analogs. Their IC50s were 80, 27, 12, and 25 μM for E3330, RN8-51, RN10-52, and RN7-60, respectively. This also shows the better functionality of the analogs in cells in comparison to E3330.

With proof that these redox-inhibiting analogs have lower IC-50 values than E3330, for both *in vitro* and in cell-based studies, we wanted to further examine the interaction they have with Ape1 using mass spectrometry analysis in hopes of gaining insight into how the reaction occurs.

Materials and Methods

Compounds

E3330 and its analogs (RN8-51, RN10-52, and RN7-60) were synthesized as previously described (*44, 46*).

Expression and purification of proteins

wtΔ40APE1

As described in Chapter II Materials and Methods.

Full-length APE1

To express and purify full-length Ape1 (FL-Apr1), an N-terminal hexa-His-SUMO-fusion (Invitrogen, Rockville, MD) was constructed. The fusion construct was transformed into Rosetta (DE3) *E. coli* (Novagen, Gibbstown, NJ), grown in 3 L of LB media with 20 µg/mL kanamycin and 34 µg/mL chloramphenicol until the OD at 600 nm reached 0.6, and then induced overnight with 1 mM isopropyl thiogalactoside at 15ºC. The cultures were harvested by centrifugation at 4000 x g for 30 min, and the pellets were stored at -80ºC. Each cell pellet was resuspended in 20 mL of 50 mM sodium phosphate buffer pH 7.8, 0.3 M NaCl, 10 mM imidazole, and then lysed by using a French press (SLM-AMINCO: Spectronic Instruments, Rochester, USA) at 1000 psi. The suspension was centrifuged at 35,000 rpm for 35 min, and the supernatant was then loaded on a Ni-NTA column at 4ºC. The column was washed with 20 column volumes of 50 mM sodium phosphate buffer pH 7.8, 0.3 M NaCl, 20 mM imidazole protein and then incubated overnight with the SUMO-specific protease Ulp1 added at a molar ratio of ~ 1:1000 (Ulp1: FL APE1). Full-length APE1 was then eluted from the column in the same

buffer and further purified using an S-Sepharose column (GE Healthcare, Piscataway, NJ) run in 50 mM MES pH 6.5, 1 mM DTT, and a linear NaCl gradient (0.05-1 M). The peak fractions were then combined, concentrated, and subjected to gel filtration chromatographic separation using a Superdex 75 (GE Healthcare, Piscataway, NJ) in 50 mM Tris pH 8.0, 0.1 M NaCl. Fractions containing full-length APE1 were then concentrated using Amicon Ultra centrifugal concentrators (Millipore, Billerica, MA) and stored at -80ºC.

Mass Spectrometric Analysis

Global ESI-QTOF Experiments

Protein samples were analyzed in the positive-ion mode on a Bruker MaXis UHR-TOF (ultra-high resolution time-of-flight) (Bruker Corp., Fremont, CA). Capillary voltage was set at -3600 V. Nebulizer pressure was 0.4 bar, and dry gas was at 1.0 L/min. The drying temperature was 180ºC. The instrument was calibrated using Tuning Mix (Agilent Technologies, Santa Clara, CA) as the external mass calibrant. Spectral deconvolution was performed using MaxEnt with Data Analysis (provided by the manufacturer of the spectrometer). Reactions of protein and redox inhibitors were carried out at a 1:5 molar ratio of protein (100 μM) to ligands (500 μM) in 10 mM HEPES (Sigma, St. Louis, MO) buffer at pH 7.5 at room temperature. Reactions were quenched on dry ice before mass spectrometry (MS) analysis. Typically, 200-300 pmol of protein samples were loaded on an Opti-Guard C18 column (10 mm × 1 mm i.d.; (Cobert Associates, St. Louis, MO) for desalting and then eluted to mass spectrometer using 50% (v/v) acetonitrile with 0.1% formic acid (FA) at 10 μL/min.

LC-MS/MS Experiments

A 10 μL solution of APE1 (100 μM) and RN6-70, RN10-52 or RN8-51 (500 μM) was incubated in 10 mM HEPES (pH 7.5) at room temperature for 0.5 h. DTT (protein/DTT = 1/20, mol/mol) was added to quench the reaction. The sample was diluted with water to a final concentration of 1 μM. A portion of the final diluted solution (50 μL) was submitted to trypsin digestion (protein/trypsin = 50/1, w/w) at 37ºC for 4 h. The solution was then analyzed by LC-MS/MS, whereby 5 μL of digestion solution was consumed for each experiment. Reversed-phase capillary LC separations were performed with an Eksigent NanoLC-1D pump (Eksigent Technologies Inc., Livermore, CA). The reversed-phase capillary column (0.075 mm × 150 mm) was packed in house by using a PicoFrit^{TM} tip (New Objective Inc., Woburn, MA) with Magic C18 resin (5 μm particles, 200 Å pore size, Michrom Bioresources Inc., Auburn, CA). The mobile phases consisted of water with 0.1% FA (A) and acetonitrile with 0.1% FA (B). Immediately after sample loading, the mobile phase was held at 98% A for 12 min. A linear gradient was performed by using 2% to 60% solvent B over 60 min, then to 80% solvent B over 10 min at 260 nL/min, followed by a 12 min re-equilibration step by 100% solvent A. The flow was directed by a PicoView Nanospray Source (PV-550, New Objective Inc., Woburn, MA) to the LTQ Orbitrap XL mass spectrometer (Thermo Fisher Scientific Inc., San Jose, CA). The spray voltage was 1.8-2.2 kV, and the capillary voltage was 27 V. The conventional data-dependent MS/MS acquisition method was employed using the Xcalibur 2.0.7 control system, in which full spectra were collected over the range of *m/z* 350–2000 followed by product-ion (MS/MS) spectra of the six most abundant ions. The full mass spectra of the peptides were acquired at high mass resolving power (60,000 for

ions of *m/z* 400) with the FT analyzer. The six most abundant precursor ions were dynamically selected in the order of highest to lowest intensity (minimal intensity of 1000 counts) and subjected to collision-induced dissociation (CID) at a normalized collision energy of 35% of the maximum available. Precursor activation was performed with an isolation width of 2 Da and an activation time of 30 ms. The automatic gain control target value was regulated at 1×10^6 for FT and 3×10^4 for the ion trap, with a maximum injection time of 1000 ms and 200 ms for the FT and the ion trap, respectively. The instrument was externally calibrated by using a standard calibration mixture of caffeine, the peptide MRFA, and Ultramark 1621 (Thermo Fisher Scientific). To identify covalent modifications, LC-MS/MS data were searched with Mascot 2.2 (Matrix Science, London, UK). Parameters used for Mascot were: enzyme, trypsin; maximum missed cleavage, 3; peptide mass tolerance, 10 ppm with one ^{13}C peak; peptide charge, +1 to +3; product mass tolerance, 0.6 Da; instrument type, default (searching for all types of b and y ions).

Results

These studies were carried out in collaboration with Michael Gross's Lab at Washington University St. Louis, specifically by Dian Su, Ph.D. We used ESI-MS to study E3330 and its analogs in a reaction with Ape1. In the experiments for FLApe1 protein, we incubated a mixture of RN7-60, RN10-52, RN8-51, and E3330, all at a 5 molar excess, for 1 minute with FLApe1. Our results, (Figure 15), show that both RN7-60 and RN10-52 form covalent adducts, but the other compounds do not. Based on the masses for RN7-60 (276 Dalton) and RN10-52 (319 Dalton) a peak shift of 240 Da and

283 Da, respectively, was seen. This difference in mass is due to the loss of HCl (36 Da) in order for a covalent reaction to occur. These analogs are the most reactive of the group, able to bind within a 1 minute time frame, and they have similar peak intensities.

Both analogs were individually tested by a 30 minute incubation with FLApe1 (Figure 16A and B). Both reactions showed all 7 cysteines to be modified, and peaks for +1 to +7 adducts were found as analyzed by LC-MS/MS following tryptic digestion.

Analog RN8-51 was further analyzed in a reaction with FLApe1 for 1 hour (Figure 16C). It only caused a partial modification; about 50% of the protein had a single cysteine modified, and 20% had a double modification. The peak shifts of 274 Da (RN8-51 has a weight of 272 Da) leads us to believe that there is no loss of substituent moieties. LC-MS/MS was again performed, and with no resulting modified peptides, we conclude the modifications that were made are reversible.

Δ40Ape1 was also tested with each compound individually with similar results: RN7-60 had +2, +3, +4, and +5 cysteines modified, RN10-52 had +2 and +3 modifications, RN8-51 only had one modification. For both FLApe1 and Δ40Ape1, with E3330 (Figure 16D) no modifications were observed.

To further probe the modifications made by RN8-51, 3 mutant forms of Δ40Ape1 were used: C99A, C138A, and C99A/C138A. These were used to determine if the modifications were only with solvent access cystienes. The samples were incubated for 3 hours before being analyzed by global MS. The double mutant had no modifications, but both single mutants had one modification each. This conclusively shows that the modifications are only occurring on the surface.

Discussion

Our results show that both RN7-60 and RN10-52 react quickly with Ape1 to form covalent adducts. All cysteines are subject to modification, and we were able to see +1 to +7 additions of these analogs to Ape1. RN8-51 only binds to the two solvent accessible cysteines (C99 and C138), and these are reversible modifications. No modifications were present for E3330. Similar results were obtained for both FLApe1 and Δ40Ape1.

In looking at Figure 17, we justify RN7-60 and RN10-52 having a more rapid Michael addition reaction because chlorine is a better leaving group, and they are able to form a covalent bond. For RN8-51, the methoxy group is a poorer leaving group than the protein thiolate, allowing the reaction to revert and making the modifications reversible.

We can conclude from this data that RN7-60 and RN10-52 are modifying more than just the solvent accessible cysteines, and so an unfolding of Ape1 must occur to expose the buried cysteines to the compounds.

As for RN8-51, it appears to behave more like E3330, forming reversible adducts with Ape1. But, in conjuction with other data (*64*), it has a lower IC50. Along with its specificity to Ape's redox function, this analog is proving to be a compound of interest for further examination in use for anti-cancer therapeutic development.

CHAPTER IV

Conclusion

In an effort to develop a novel cancer therapeutic, Ape1 is an attractive target because it has two important functions, BER and redox. Our research focused on the redox function of Ape1, which would prevent cell proliferation. Other studies have shown that intracellular redox could be used as regulator of growth in cancer cells (*35*). Regulation of the intracellular redox environment is critical for cell viability and maintenance of cellular homeostasis. An Ape1 deficient human cell line cannot be generated because Ape1 is essential for early embryonic development (*39*). Therefore, identification and development of a specific inhibitor of this protein will significantly help as a tool in Ape1 functional study and therapeutic potential.

Our studies, divided into two parts, examined the inhibitors that block Ape1 redox function. The first section uses E3330 because of its ability to kill a variety of cancer cells without significantly affecting normal cells (*44*). Using this inhibitor, we conducted a series of experiments to examine the Ape1 redox mechanism.

We developed a chemical footprinting/mass spectrometric assay using to characterize the interaction of the redox inhibitor, E3330, with Ape1. Our results show an interaction between E3330 and Ape1 and allow us to conclude that Ape1 requires a conformational change in order to obtain the +7 NEM adduct. This chemical footprinting combined with the HDX kinetics gives strong evidence for the existence of a partially or locally unfolded conformation of Ape1. The unfolding in our experiments helps us to

explain the exposure for the buried residue Cys65, which was previously shown to be required for redox function.

In our search for understanding the mechanism by which E3330 inhibits the redox activity of Ape1, we propose that E3330 interacts with the locally unfolded state of Ape1, stabilizing it so that the normally buried Cys residues can react with NEM in our experiments. In shifting the equilibrium toward the locally unfolded state of Ape1, E3330 also increases disulfide bond formation in Ape1. This increase could be due to a stabilization of the unfolded conformation by E3330 or due to a reversible modification of Cys residues, making them susceptible to nucleophilic attack by a sylfhydryl and thereby resulting in disulfide bond formation.

The third chapter includes a characterization of analog compounds of E3330: RN7-60, RN8-51, and RN10-52. These compounds were in a recent publication (*46*), and further investigation was necessary to determine their value as redox inhibitors and to assess whether they were an improvement over E3330. The analogs also provide further information regarding Ape1's redox function.

Other studies have shown that these redox-inhibiting analogs have lower IC-50 values than E3330, for both in vitro and in cell-based studies. We can conclude from this data that RN7-60 and RN10-52 are modifying more than just the solvent accessible cysteines, and so an unfolding of Ape1 must occur to expose the buried cysteines to the compounds.

And for RN8-51, it appears to behave more like E3330, forming reversible adducts with Ape1. But, in conjuction with other data (*64*), it has a lower IC50. Along

with its specificity to Ape's redox function, this analog is proving to be a compound of interest for further examination in use for anti-cancer therapeutic development.

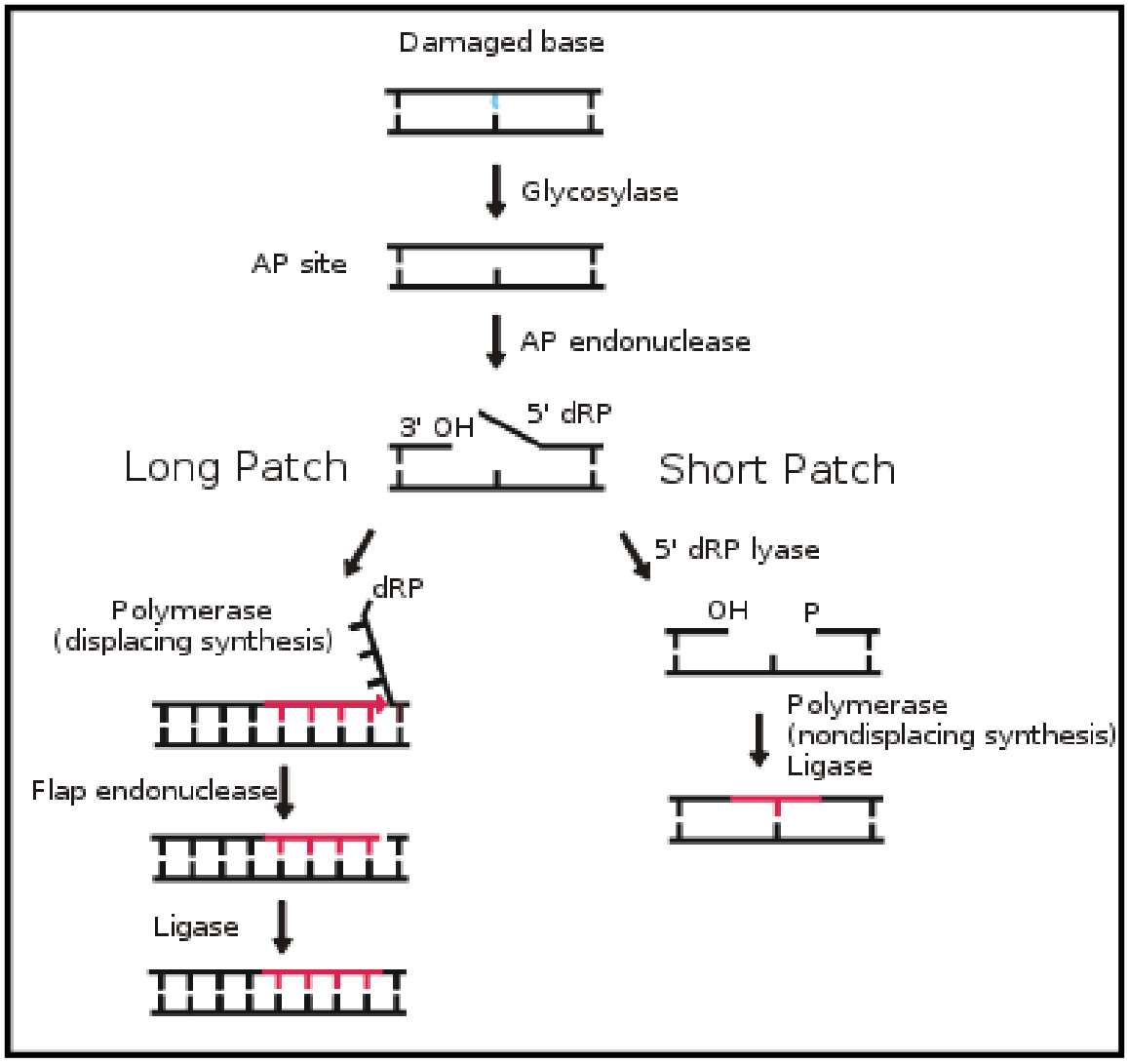

Figure 1 BER pathway. Ape1 is the AP endonuclease that cleaves abasic sites in the second step of the Base Excision Repair pathway.

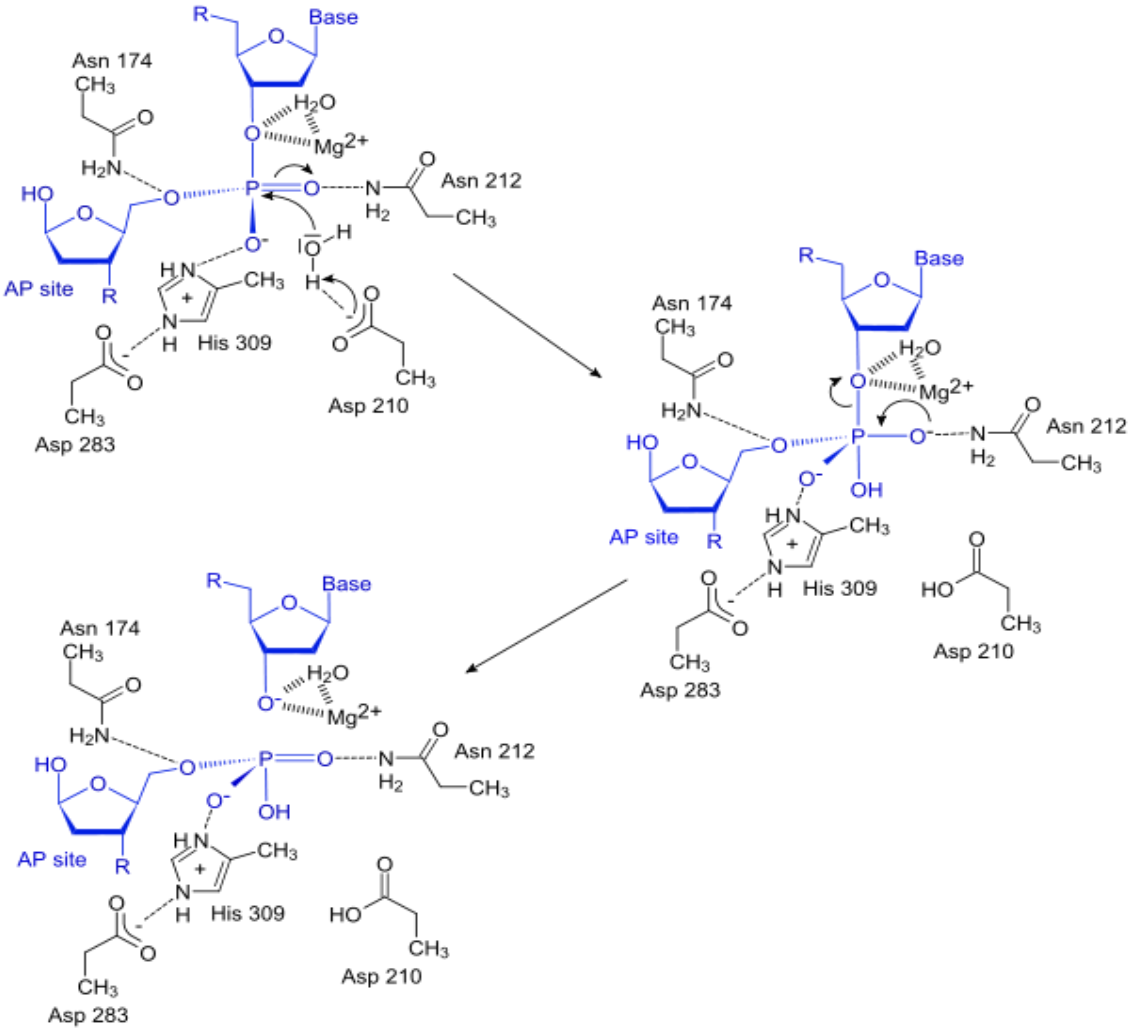

Figure 2 Ape1's role in BER pathway. Figure from Tainer, J. et al *Nature* **403** (6768): 451–456. Ape1 plays a critical role in the BER DNA repair pathway as an AP endonuclease, which processes the AP sites. Ape1's role in the BER pathway begins when the Ape1 enzyme creates a nick in the phosphodiester backbone at a abasic (baseless) site through acyl substitution. The Asp210 residue deprotonates a water molecule, which then performs a nucleophilic attack on the phosphate group located 5´ to the AP site. Electrons from an oxygen atom in the phosphate group moves down, freeing a 5´ phosphate group on the AP site and a 3´-OH on the normal nucleotide, both of which are stabilized by the Mg^{2+} ion.

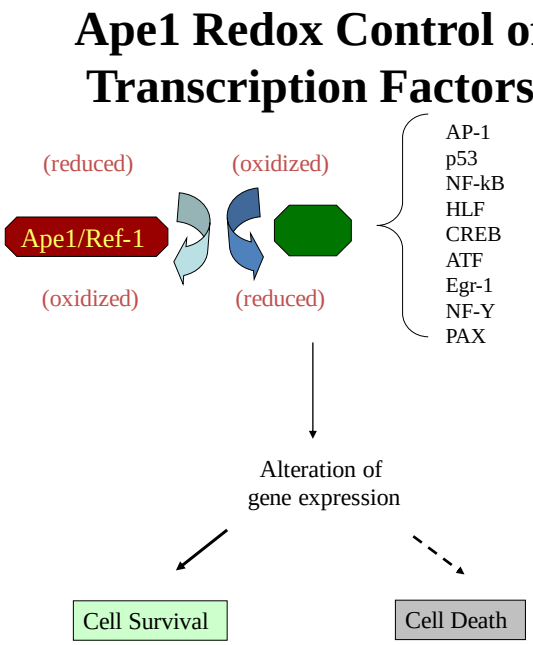

Figure 3 Ape1's role in redox of transcription factors. Through its redox function, Ape1 regulates gene expression by modifying the redox status of some transcription factors which are involved in variety of cancer processes. The redox control of transcription factors alters gene expression, leading to cell survival or cell death.

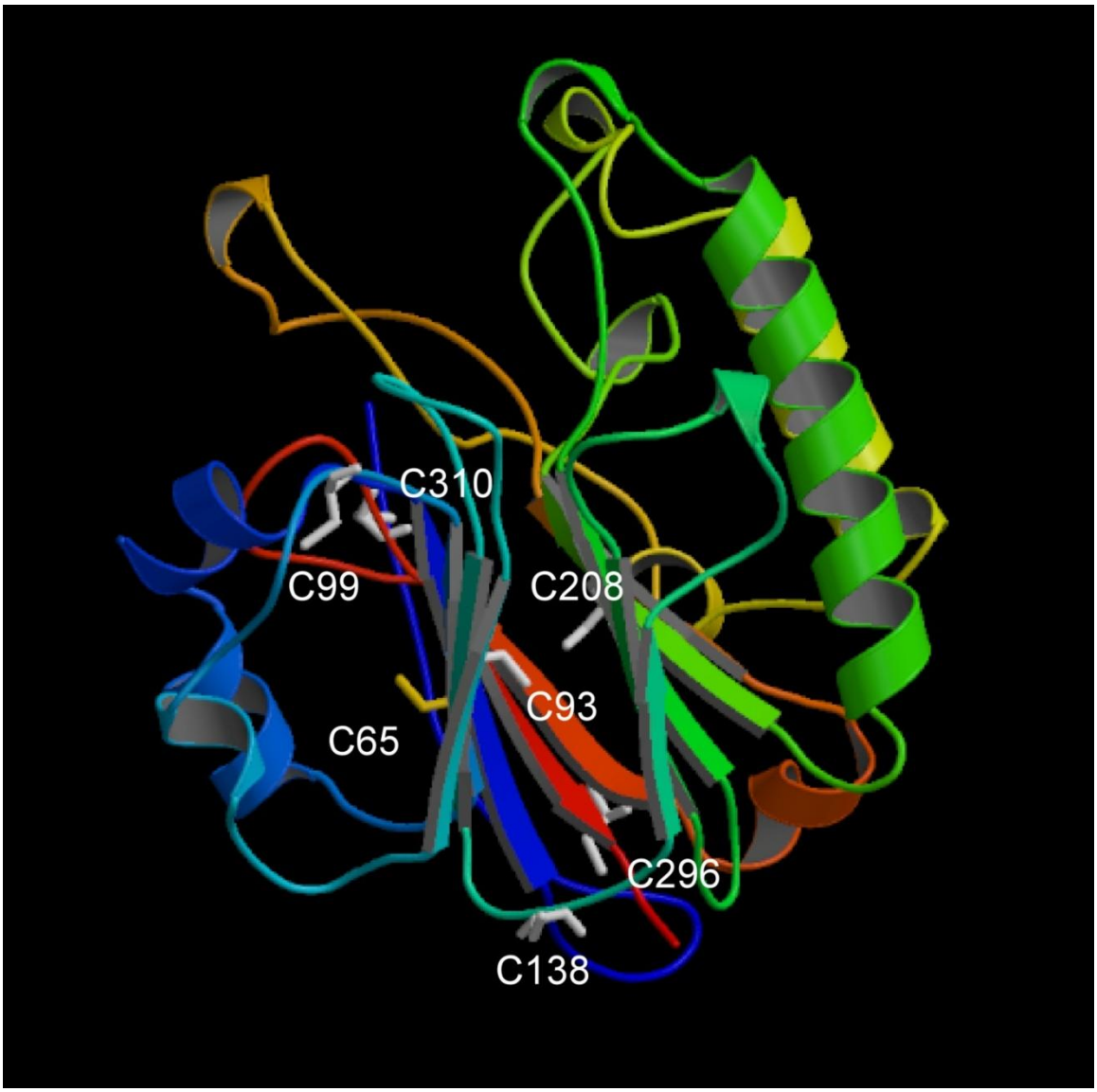

Figure 4 X-ray crystal structure of Ape1. X-ray crystal structure of hApe1 with seven cysteines shown. C99 and C138 are surface accessible, whereas C65, C93, C208, C296, and C310 are buried. C65 is thought to be essential in the redox function of the protein.

E3330
Molecular Weight:
378.8

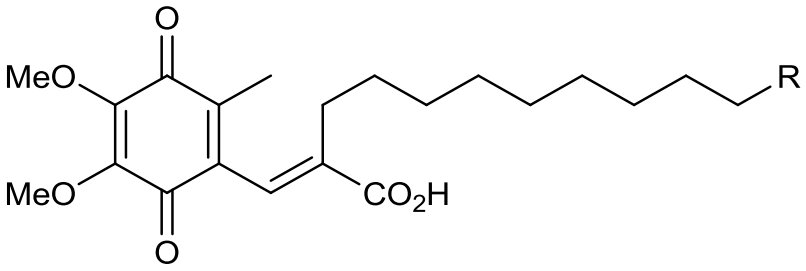

NEM
Molecular Weight:
125.1

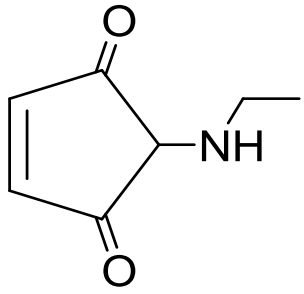

Figure 5 Chemical structures of E3330 and NEM.

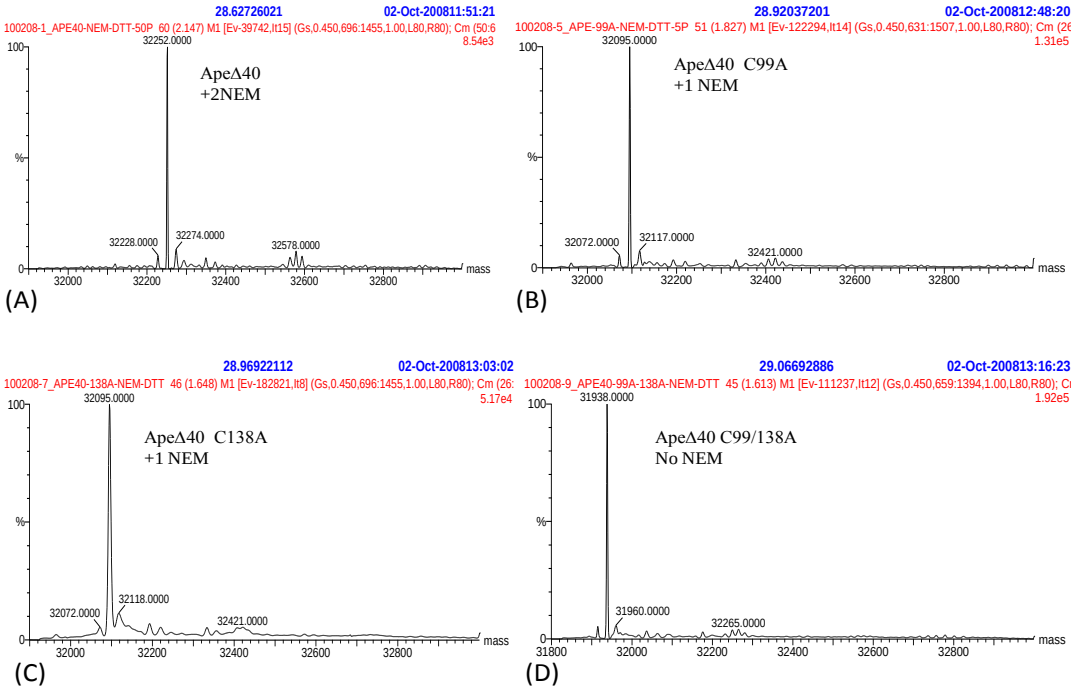

Figure 6 ESI mass spectra wtΔ40Ape1 and mutants with NEM labeling. wtΔ40Ape1 and the 3 mutants (C99A, C138A, C99A/C138A) were incubated with NEM and without E3330 to verify the labeling that would occur for Ape1 untreated with E3330. wtΔ40Ape1 results in the formation of a +2 NEM modified species as indicated by a shift in mass of 250 Da (A). The C99A and C138A show a reduction from +2 NEM for wtΔ40Ape1 to +1 NEM (B and C), and for the double mutant there is no longer any NEM bound (D). These products form within 30 s of the addition of NEM.

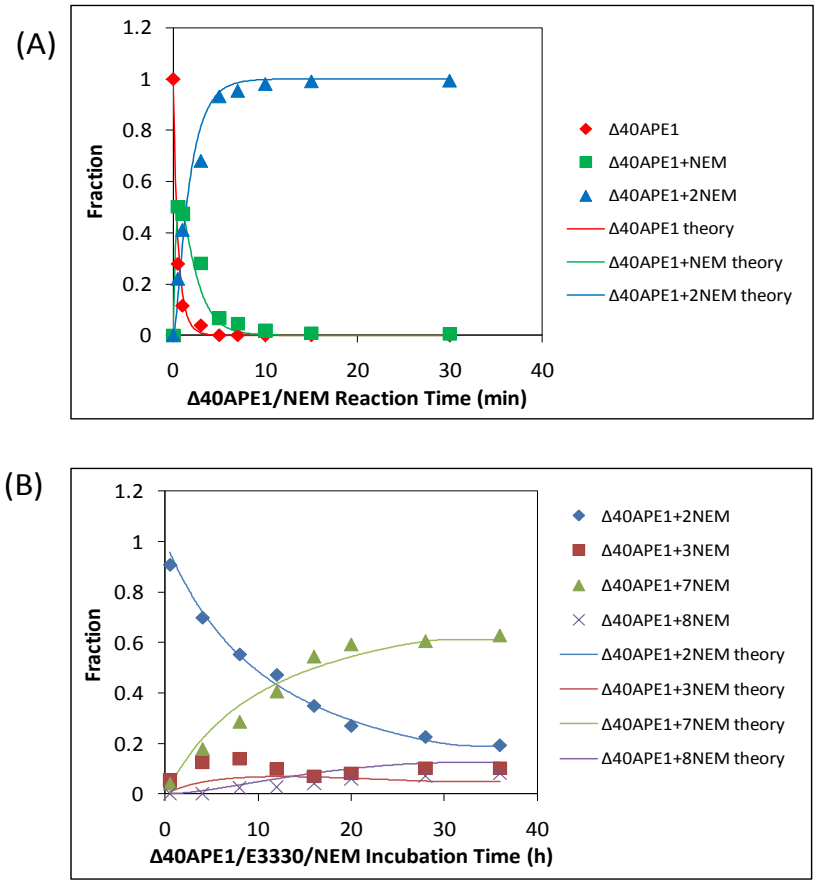

Figure 7 Kinetics of wtΔ40Ape1 with E3330 and NEM. Kinetics of wtΔ40Ape1 reaction with NEM (A) or NEM and E3330 (B). Both samples were prepared in 10 mM HEPES at pH 7.5 at RT ([protein] = 100 µM; [E3330] = [NEM] = 500 µM). Aliquots were quenched with DTT at various times. Mass spectra were collected on a Bruker MaXis UHR-TOF instrument, and deconvolution was done with MaxEnt1 algorithm provided with that system. The sums of intensities of different NEM adducts of Δ40APE1 were normalized to 1. Data were fitted with Mathcad using a relatively straight forward one-parameter fit of the +2 NEM adduct kinetic curves and a three parameter fit varying k^{slow}_{NEM} , $k_{ON,}$ *and* g_N was used to fit the +7 NEM adduct kinetic curves.

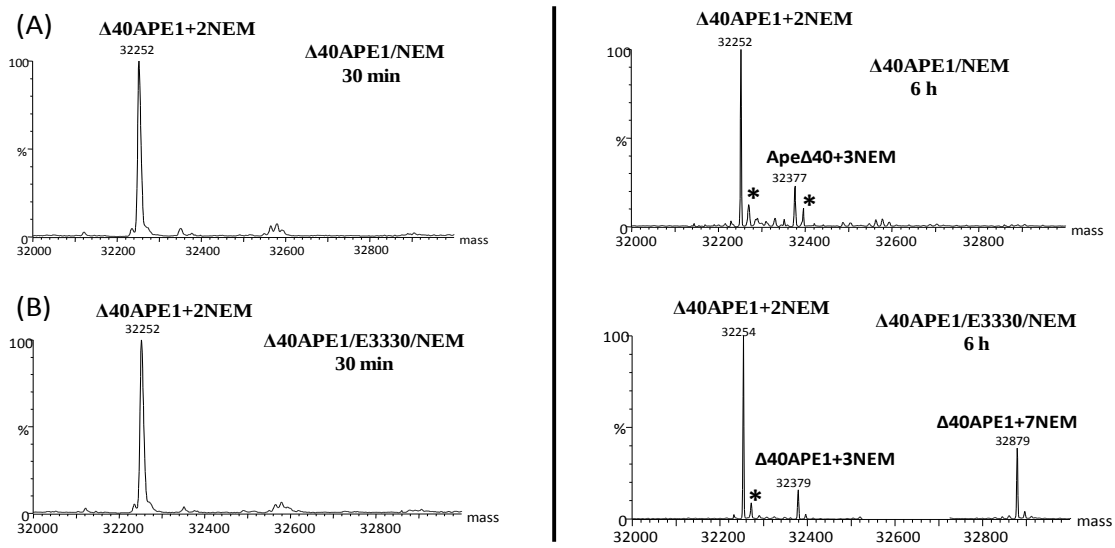

Figure 8 ESI mass spectra of wtΔ40Ape1 with E3330 and NEM. ESI mass spectra of wtΔ40Ape1 after incubation without (A) and with E3330 (B) in the presence of NEM for 30 min (left panel) and 6 h (right panel). Samples were incubated in 10 mM HEPES with 150 mM KCl at pH 7.5([protein] = 100 μM; [E3330] = [NEM] = 500 μM). The symbol * denotes peaks for the water adducts. Mass spectra were collected on a Waters Micromass Q-TOF instrument and deconvolution was done with MaxEnt1 algorithm provided with that system.

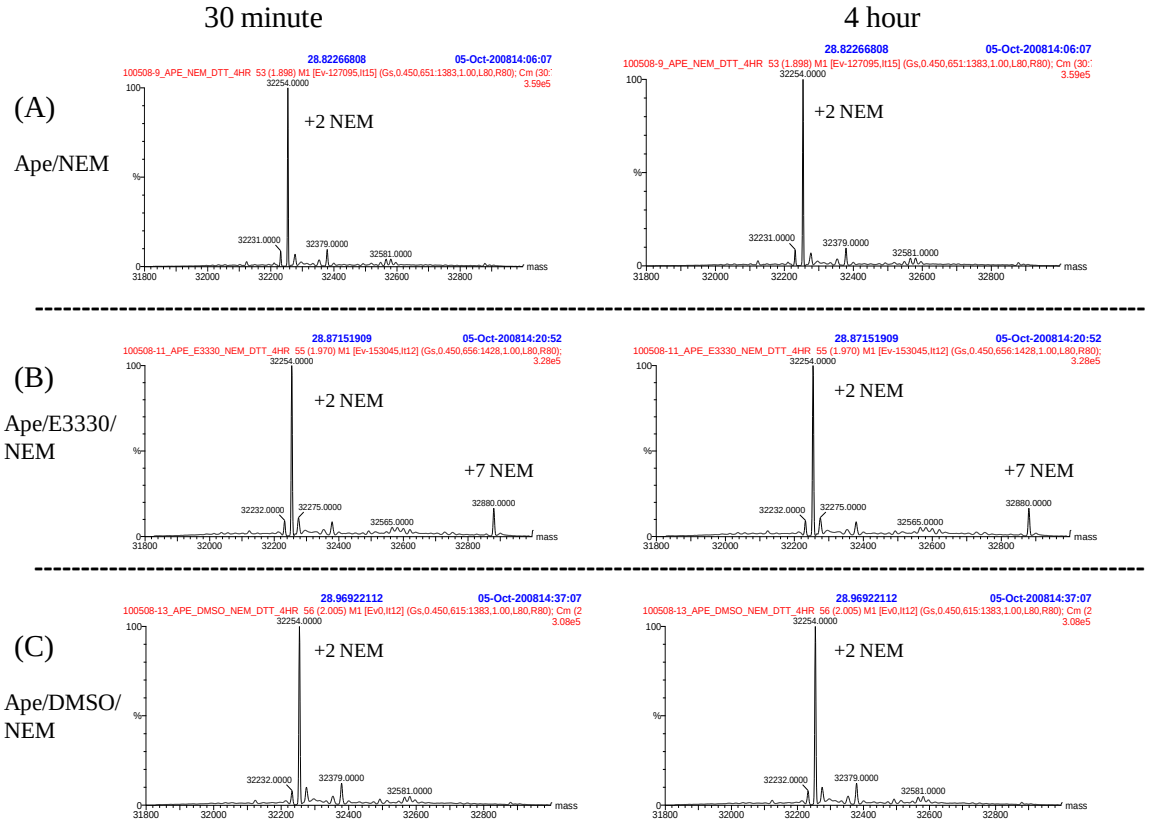

Figure 9 ESI mass spectra of wtΔ40Ape1 at 30 min and 4 hr. ESI mass spectra of reactions with (A) wtΔ40Ape1/NEM alone, (B) with E3330, and (C) with DMSO were incubate at 30 minutes and 4 hour then analyzed on a Waters Micromass Q-TOF instrument and deconvolution was done with MaxEnt1 algorithm provided with that system. At 30 min, all three samples appeared identical with a +2 NEM. At 4 hours, all samples still have the same +2 NEM peak; however, they also have a small +3 NEM peak. The E3330 sample also includes a +7 NEM peak.

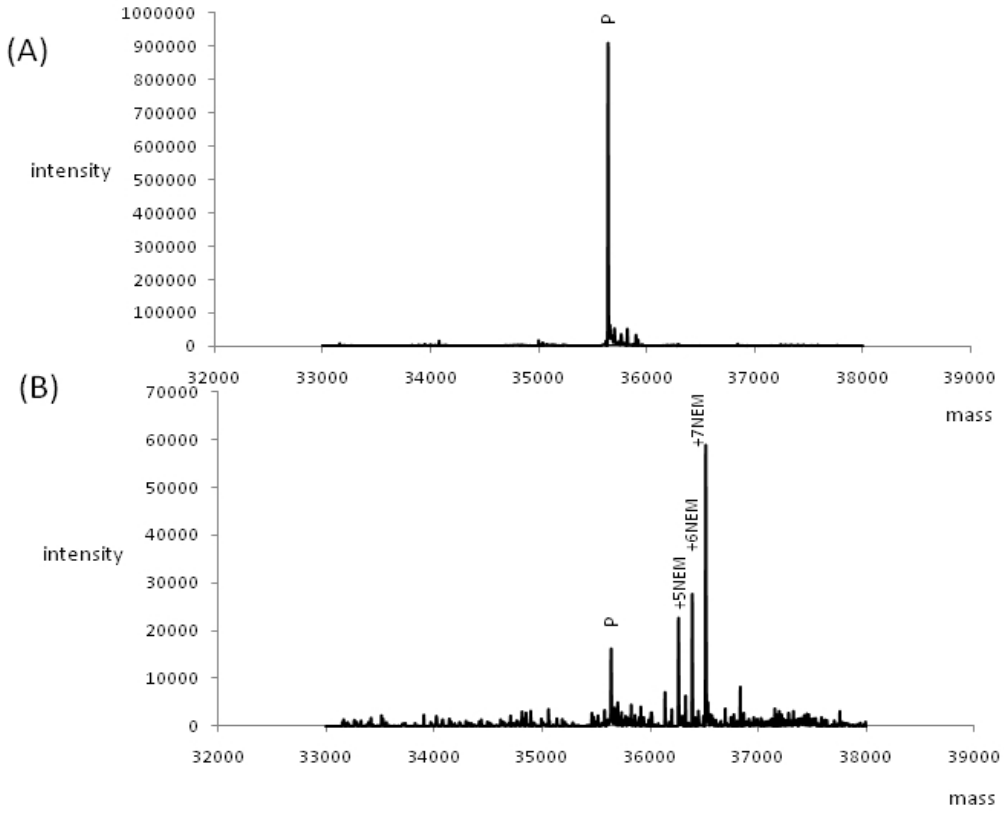

Figure 10 ESI mass spectra of denatured FLApe with NEM. ESI mass spectra of untreated native full-length Ape1 (A) and denatured full-length Ape1 treated with NEM (B). In (A), the only major peak is the parent peak for full-length Ape1 labeled P with an observed mass of 35,641.3 (expected 35,641.5). Treatment of denatured Ape1 (B) resulted in 4 major peaks including the parent peak labeled P, along with +5 (36,266.6), +6 (36,392.4), and +7 (36,517.3) NEM modifications to the parent molecule. No higher mass peaks for modification with NEM beyond +7 NEM were observed.

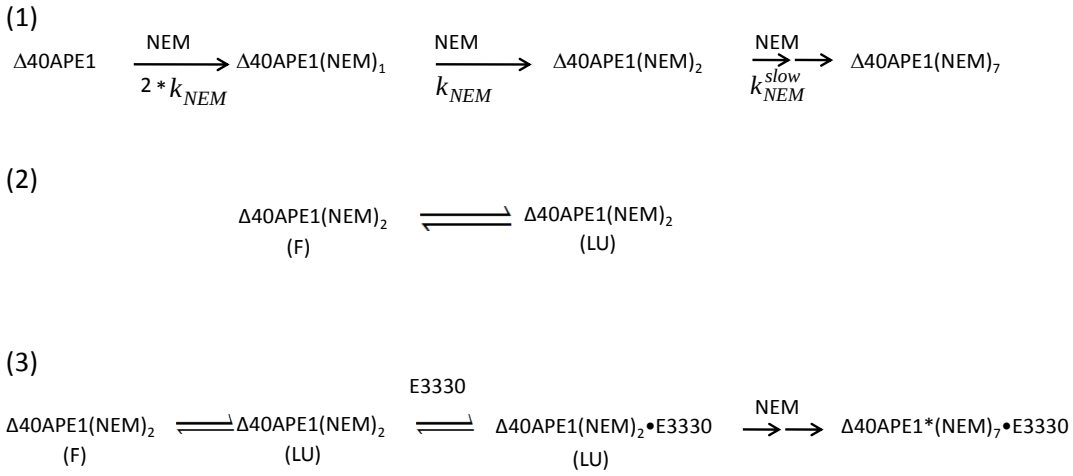

Figure 11 Scheme of Ape1 unfolding. The reaction of wtΔ40Ape1 with NEM in the presence or absence of E3330 involves several intermediates. The initial reaction of wtΔ40Ape1 with NEM is rapid for the +2 NEM molecules. Then there is a slower reaction to modify all seven Cys residues of wtΔ40Ape1. The rate-limiting step for the reaction is a conformational change of the +2 NEM species from a fully folded state to a locally unfolded state. E3330 then binds to and stabilizes this locally unfolded state, allowing the exposure of one or more buried Cys residues. These exposed residues can then react with NEM, leading to the +7 NEM modified species.

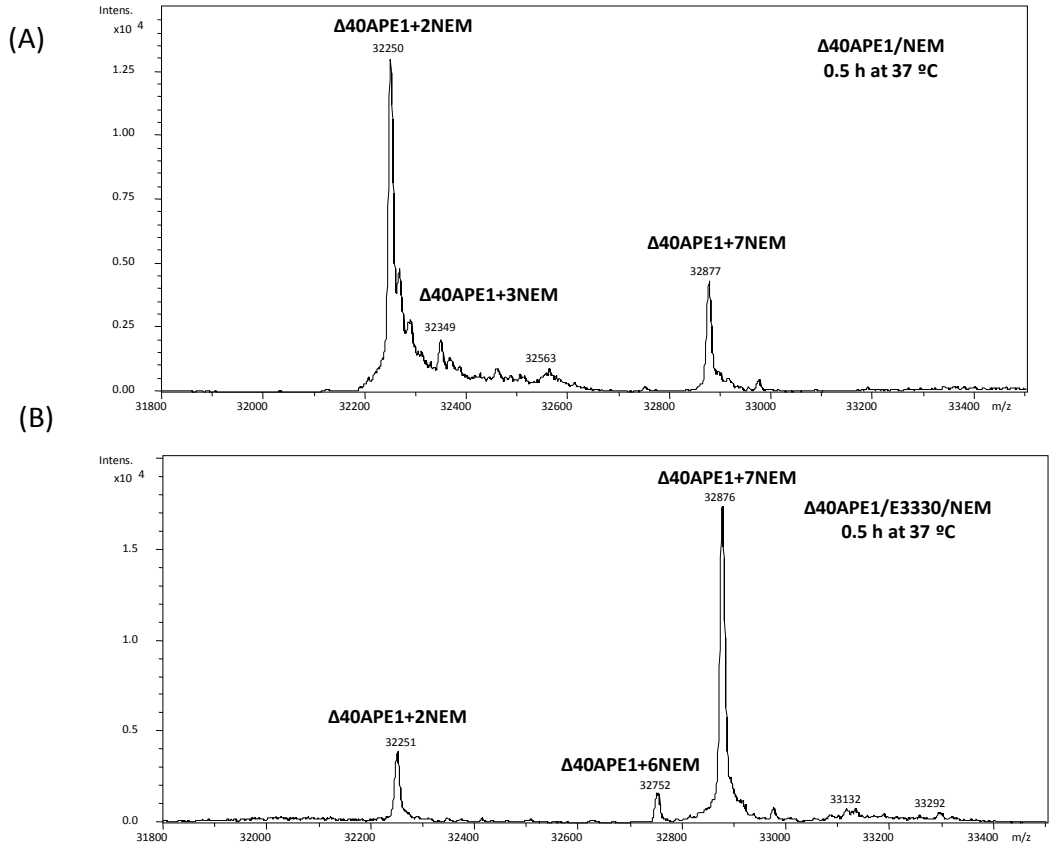

Figure 12 ESI mass spectra wtΔ40Ape1 increased temperature. ESI mass spectra of wtΔ40Ape1 without and with incubation with E3330 in the presence of NEM for 0.5 h at 37 ºC. Sample was incubated in 10 mM HEPES at pH 7.5 ([protein] = 10 µM; [E3330] = [NEM] = 50 µM). Mass spectrum was collected on a Bruker MaXis UHR-TOF instrument and deconvolution was done with MaxEnt1 algorithm.

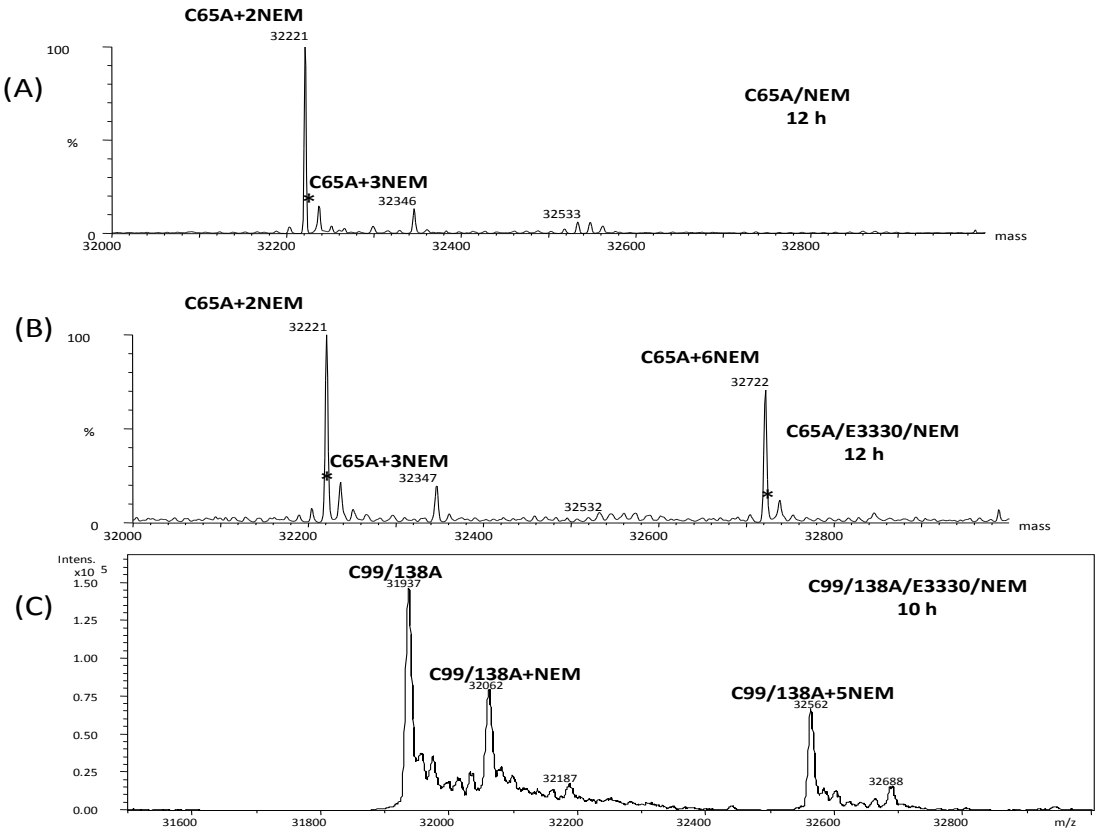

Figure 13 ESI mass spectra of hΔ40Ape1 mutants. ESI mass spectra of C65A Δ40Ape1 without (A) and with incubation with E3330 (B) in the presence of NEM for 12 h. (C) ESI mass spectra of C99A/C138A Δ40Ape1 incubated with E3330 and NEM for 12 h. Samples were incubated in 10 mM HEPES at pH 7.5 ([protein] = 100 μM; [E3330] = [NEM] = 500 μM). The symbol * denotes water adducts. Mass spectra were collected on a Waters Micromass Q-TOF instrument and deconvolution was done with MaxEnt1 algorithm that was part of that system.

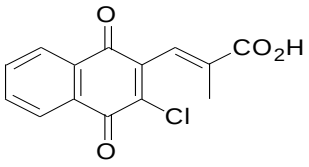

RN7-60b

Molecular Weight:
242.2

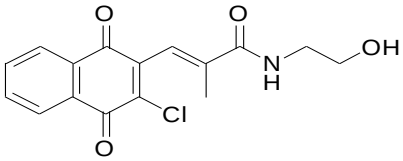

RN10-52

Molecular Weight:
285.2

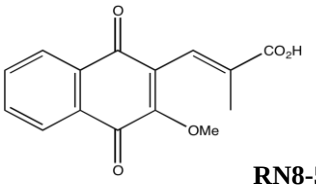

RN8-51

Molecular Weight:
237.8

Figure 14 Chemical structures of E3330 analogs: RN7-60b, RN10-52, and RN8-51.

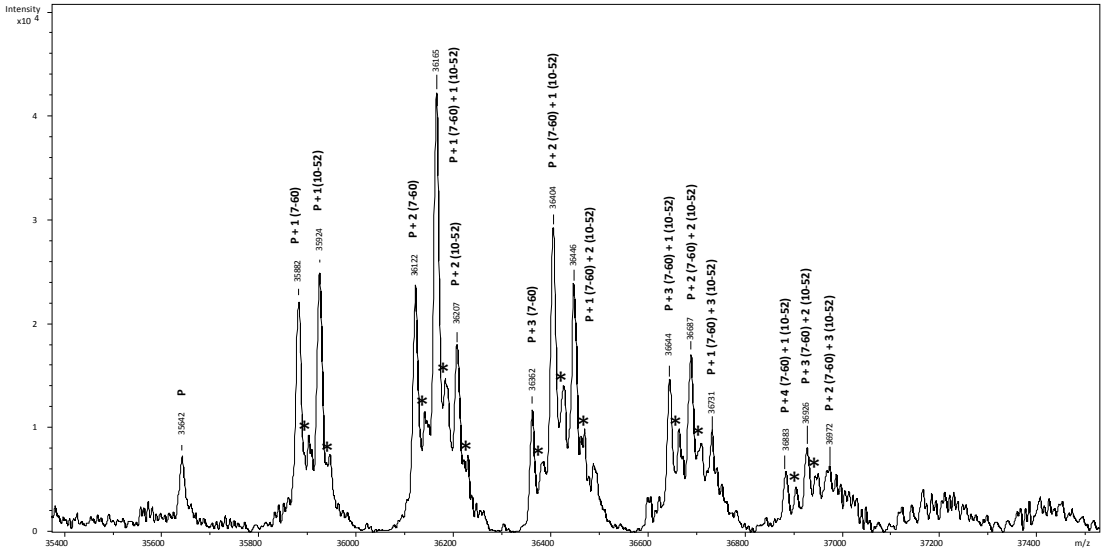

Figure 15 ESI mass spectra of FLApe1 and all E3330 compounds. ESI spectrum of FL-Ape1 and mixture of ligands (RN7-60, RN10-52, RN8-51, and E3330) after 1-min reaction showing modifications by RN7-60 and RN10-52. P stands for FL-APE1; * indicates the water adducts of the protein and ligand complexes.

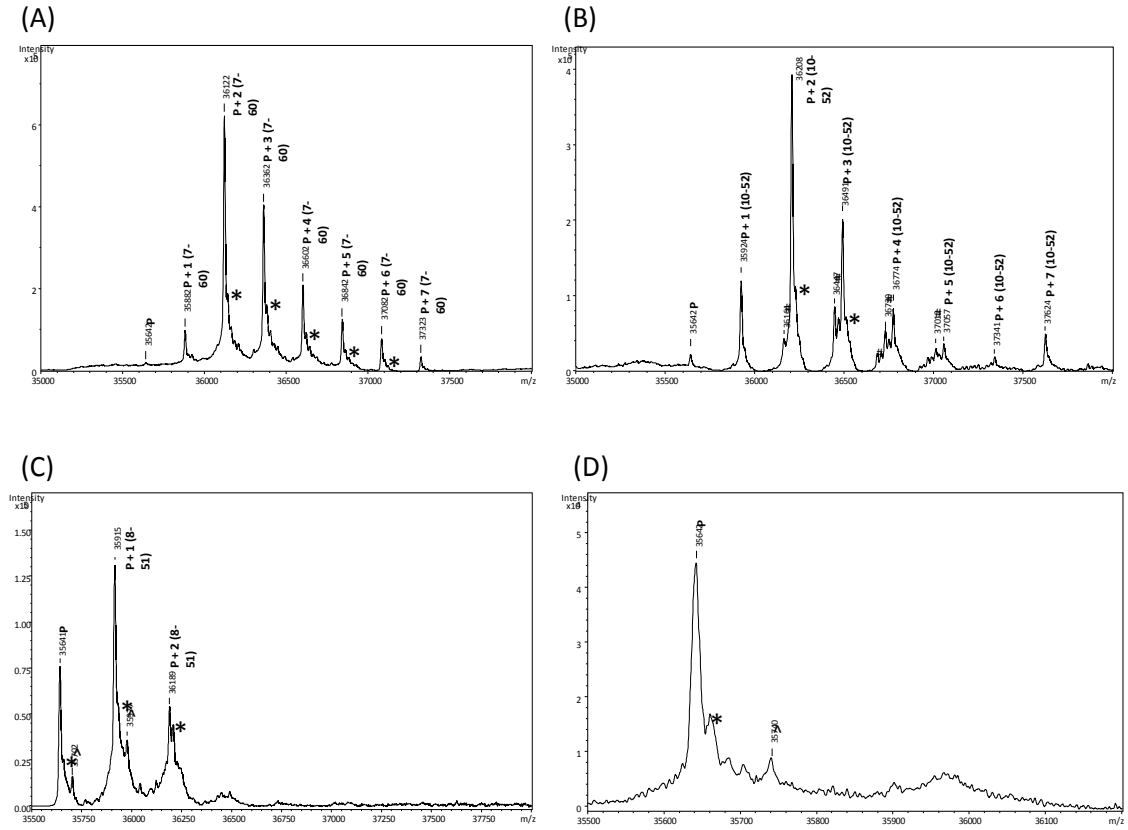

Figure 16 ESI mass spectra of FLApe1 and analogs showing modification. ESI spectra of FL-Ape1 and (A) RN7-60 and (B) 10-52 after 0.5-h reaction showing multiple (1, 2, 3, 4, 5, 6, and 7) modifications. (C) ESI spectra of FL-Ape1 and RN8-51 after 1-h reaction showing 1 and 2 modifications. (D) ESI spectra of FL-Ape1 and E3330 after 2-hour reaction showing no modifications by E3330. P stands for FL-Ape1; * indicates the water adducts of the protein and ligand complexes; # indicates the contamination peaks due to the carry-overs on the C18 guard column. ^ indicates unidentified peaks.

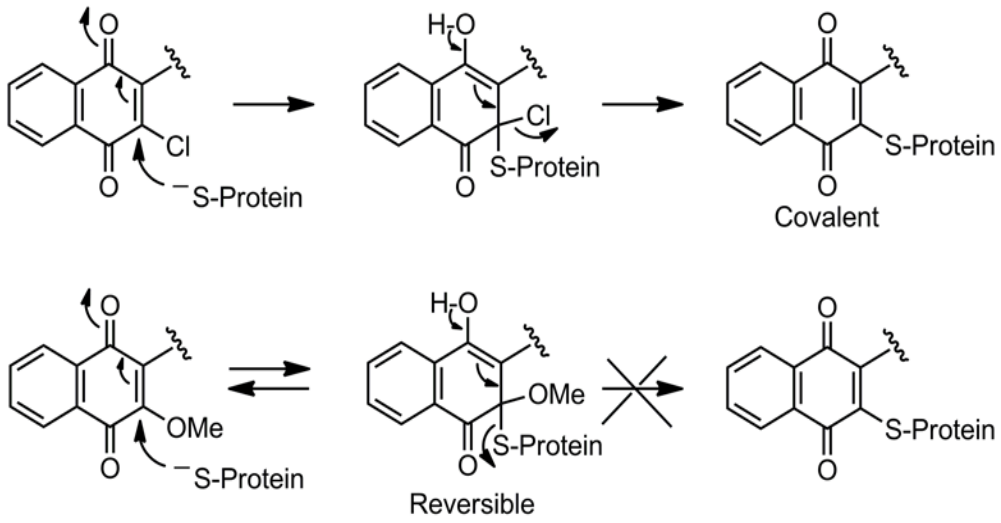

Figure 17 Mechanism of covalent vs. reversible inhibition of Ape1 redox activity.

References

1. Luo, M., He, H., Kelley, M. R., and Georgiadis, M. M. (2010) Redox regulation of DNA repair: implications for human health and cancer therapeutic development, *Antioxid Redox Signal 12*, 1247-1269.
2. Xanthoudakis, S., Smeyne, R. J., Wallace, J. D., and Curran, T. (1996) The redox/DNA repair protein, Ref-1, is essential for early embryonic development in mice, *Proc Natl Acad Sci U S A 93*, 8919-8923.
3. Xanthoudakis, S., Miao, G. G., and Curran, T. (1994) The redox and DNA-repair activities of Ref-1 are encoded by nonoverlapping domains, *Proc Natl Acad Sci U S A 91*, 23-27.
4. Altieri, F., Grillo, C., Maceroni, M., and Chichiarelli, S. (2008) DNA damage and repair: from molecular mechanisms to health implications, *Antioxid Redox Signal 10*, 891-937.
5. Christmann, M., Tomicic, M. T., Roos, W. P., and Kaina, B. (2003) Mechanisms of human DNA repair: an update, *Toxicology 193*, 3-34.
6. Evans, A. R., Limp-Foster, M., and Kelley, M. R. (2000) Going APE over Ref-1, *Mutat Res 461*, 83-108.
7. Demple, B., and Harrison, L. (1994) Repair of oxidative damage to DNA: enzymology and biology, *Annu Rev Biochem 63*, 915-948.
8. Doetsch, P. W., and Cunningham, R. P. (1990) The enzymology of apurinic/apyrimidinic endonucleases, *Mutat Res 236*, 173-201.
9. Barzilay, G., Mol, C. D., Robson, C. N., Walker, L. J., Cunningham, R. P., Tainer, J. A., and Hickson, I. D. (1995) Identification of critical active-site residues in the multifunctional human DNA repair enzyme HAP1, *Nat Struct Biol 2*, 561-568.
10. Chen, D. S., Herman, T., and Demple, B. (1991) Two distinct human DNA diesterases that hydrolyze 3'-blocking deoxyribose fragments from oxidized DNA, *Nucleic Acids Res 19*, 5907-5914.
11. David, S. S., and Williams, S. D. (1998) Chemistry of Glycosylases and Endonucleases Involved in Base-Excision Repair, *Chem Rev 98*, 1221-1262.
12. Wilson, T. M., Rivkees, S. A., Deutsch, W. A., and Kelley, M. R. (1996) Differential expression of the apurinic / apyrimidinic endonuclease (APE/ref-1) multifunctional DNA base excision repair gene during fetal development and in adult rat brain and testis, *Mutat Res 362*, 237-248.
13. Curran, T., and Franza, B. R., Jr. (1988) Fos and Jun: the AP-1 connection, *Cell 55*, 395-397.
14. Xanthoudakis, S., and Curran, T. (1992) Identification and characterization of Ref-1, a nuclear protein that facilitates AP-1 DNA-binding activity, *EMBO J 11*, 653-665.
15. Abate, C., Luk, D., and Curran, T. (1990) A ubiquitous nuclear protein stimulates the DNA-binding activity of fos and jun indirectly, *Cell Growth Differ 1*, 455-462.

16. Xanthoudakis, S., Miao, G., Wang, F., Pan, Y. C., and Curran, T. (1992) Redox activation of Fos-Jun DNA binding activity is mediated by a DNA repair enzyme, *EMBO J 11*, 3323-3335.
17. Abate, C., Patel, L., Rauscher, F. J., 3rd, and Curran, T. (1990) Redox regulation of fos and jun DNA-binding activity in vitro, *Science 249*, 1157-1161.
18. Abate, C., Luk, D., Gentz, R., Rauscher, F. J., 3rd, and Curran, T. (1990) Expression and purification of the leucine zipper and DNA-binding domains of Fos and Jun: both Fos and Jun contact DNA directly, *Proc Natl Acad Sci U S A 87*, 1032-1036.
19. Hirota, K., Matsui, M., Iwata, S., Nishiyama, A., Mori, K., and Yodoi, J. (1997) AP-1 transcriptional activity is regulated by a direct association between thioredoxin and Ref-1, *Proc Natl Acad Sci U S A 94*, 3633-3638.
20. Hirota, K., Murata, M., Sachi, Y., Nakamura, H., Takeuchi, J., Mori, K., and Yodoi, J. (1999) Distinct roles of thioredoxin in the cytoplasm and in the nucleus. A two-step mechanism of redox regulation of transcription factor NF-kappaB, *J Biol Chem 274*, 27891-27897.
21. Ueno, M., Masutani, H., Arai, R. J., Yamauchi, A., Hirota, K., Sakai, T., Inamoto, T., Yamaoka, Y., Yodoi, J., and Nikaido, T. (1999) Thioredoxin-dependent redox regulation of p53-mediated p21 activation, *J Biol Chem 274*, 35809-35815.
22. Ema, M., Hirota, K., Mimura, J., Abe, H., Yodoi, J., Sogawa, K., Poellinger, L., and Fujii-Kuriyama, Y. (1999) Molecular mechanisms of transcription activation by HLF and HIF1alpha in response to hypoxia: their stabilization and redox signal-induced interaction with CBP/p300, *Embo J 18*, 1905-1914.
23. Lando, D., Pongratz, I., Poellinger, L., and Whitelaw, M. L. (2000) A redox mechanism controls differential DNA binding activities of hypoxia-inducible factor (HIF) 1alpha and the HIF-like factor, *J Biol Chem 275*, 4618-4627.
24. Cao, X., Kambe, F., Ohmori, S., and Seo, H. (2002) Oxidoreductive modifcation of two cyteine residues in paired domain by Ref-1 regulates DNA-binding activity of Pax-8, *Biochem. Biophys. Res. Commun. 297*, 288-293.
25. Tell, G., Zecca, A., Pellizzari, L., Spessotto, P., Colombatti, A., Kelley, M. R., Damante, G., and Pucillo, C. (2000) An 'environment to nucleus' signaling system operates in B lymphocytes: redox status modulates BSAP/Pax-5 activation through Ref-1 nuclear translocation, *Nucleic Acids Res 28*, 1099-1105.
26. Mol, C. D., Izumi, T., Mitra, S., and Tainer, J. A. (2000) DNA-bound structures and mutants reveal abasic DNA binding by APE1 and DNA repair coordination [corrected], *Nature 403*, 451-456.
27. Gorman, M. A., Morera, S., Rothwell, D. G., La Fortelle, E., Mol, C. D., Tainer, J. A., Hickson, I. D., and Freemont, P. S. (1997) The crystal structure of the human DNA repair endonuclease HAP1 suggests the recognition of extra-helical deoxyribose at DNA abasic sites., *EMBO J 16*, 6548-6558.
28. Beernink, P. T., Segelke, B. W., Hadi, M. Z., Erzberger, J. P., Wilson, D. M., 3rd, and Rupp, B. (2001) Two divalent metal ions in the active site of a new crystal form of human apurinic/apyrimidinic endonuclease, Ape1: implications for the catalytic mechanism, *J Mol Biol 307*, 1023-1034.

29. Georgiadis, M. M., Luo, M., Gaur, R. K., Delaplane, S., Li, X., and Kelley, M. R. (2008) Evolution of the redox function in mammalian apurinic/apyrimidinic endonuclease, *Mutat Res 643*, 54-63.
30. Xanthoudakis, S., and Curran, T. (1996) Redox regulation of AP-1: a link between transcription factor signaling and DNA repair, *Adv Exp Med Biol 387*, 69-75.
31. Walker, L. J., Robson, C. N., Black, E., Gillespie, D., and Hickson, I. D. (1993) Identification of residues in the human DNA repair enzyme HAP1 (Ref-1) that are essential for redox regulation of Jun DNA binding, *Mol Cell Biol 13*, 5370-5376.
32. Ordway, J. M., Eberhart, D., and Curran, T. (2003) Cysteine 64 of Ref-1 is not essential for redox regulation of AP-1 DNA binding., *Mol. Cell. Biol. 23*, 4257-4266.
33. Havelka, A. M., Berndtsson, M., Olofsson, M. H., Shoshan, M. C., and Linder, S. (2007) Mechanisms of action of DNA-damaging anticancer drugs in treatment of carcinomas: is acute apoptosis an "off-target" effect?, *Mini Rev Med Chem 7*, 1035-1039.
34. Fishel, M. L., and Kelley, M. R. (2007) The DNA base excision repair protein Ape1/Ref-1 as a therapeutic and chemopreventive target, *Mol Aspects Med 28*, 375-395.
35. Harris, A. L. (2002) Hypoxia--a key regulatory factor in tumour growth, *Nat Rev Cancer 2*, 38-47.
36. Kelley, M. R., Cheng, L., Foster, R., Tritt, R., Jiang, J., Broshears, J., and Koch, M. (2001) Elevated and altered expression of the multifunctional DNA base excision repair and redox enzyme Ape1/ref-1 in prostate cancer, *Clin Cancer Res 7*, 824-830.
37. Sak, S. C., Harnden, P., Johnston, C. F., Paul, A. B., and Kiltie, A. E. (2005) APE1 and XRCC1 protein expression levels predict cancer-specific survival following radical radiotherapy in bladder cancer, *Clin Cancer Res 11*, 6205-6211.
38. McNeill, D. R., and Wilson, D. M., 3rd. (2007) A dominant-negative form of the major human abasic endonuclease enhances cellular sensitivity to laboratory and clinical DNA-damaging agents, *Mol Cancer Res 5*, 61-70.
39. Madhusudan, S., and Middleton, M. R. (2005) The emerging role of DNA repair proteins as predictive, prognostic and therapeutic targets in cancer, *Cancer Treat Rev 31*, 603-617.
40. Kelley, M. R., and Fishel, M. L. (2008) DNA repair proteins as molecular targets for cancer therapeutics, *Anticancer Agents Med Chem 8*, 417-425.
41. Shimizu, N., Sugimoto, K., Tang, J., Nishi, T., Sato, I., Hiramoto, M., Aizawa, S., Hatakeyama, M., Ohba, R., Hatori, H., Yoshikawa, T., Suzuki, F., Oomori, A., Tanaka, H., Kawaguchi, H., Watanabe, H., and Handa, H. (2000) High-performance affinity beads for identifying drug receptors, *Nat Biotechnol 18*, 877-881.
42. Zou, G. M., Luo, M. H., Reed, A., Kelley, M. R., and Yoder, M. C. (2007) Ape1 regulates hematopoietic differentiation of embryonic stem cells through its redox functional domain, *Blood 109*, 1917-1922.

43. Zou, G. M., and Maitra, A. (2008) Small-molecule inhibitor of the AP endonuclease 1/REF-1 E3330 inhibits pancreatic cancer cell growth and migration, *Mol Cancer Ther 7*, 2012-2021.
44. Luo, M., Delaplane, S., Jiang, A., Reed, A., He, Y., Fishel, M., Nyland II, R. L., Borch, R. F., Qiao, X., Georgiadis, M. M., and Kelley, M. R. (2008) Role of the multifunctional DNA repair and redox signaling protein Ape1/Ref-1 in cancer and endothelial cells: Small molecule inhibition of Ape1's redox function, *Antioxid Redox Signal 10*, 1853-1867.
45. Su, D., Delaplane, S., Luo, M., Rempel, D. L., Vu, B., Kelley, M. R., Gross, M. L., and Georgiadis, M. M. (2011) Interactions of Apurinic/Apyrimidinic Endonuclease with a Redox Inhibitor: Evidence for an Alternate Conformation of the Enzyme, *Biochemistry 50*, 82-99.
46. Nyland, R. L., Luo, M., Kelley, M. R., and Borch, R. F. (2010) Design and synthesis of novel quinone inhibitors targeted to the redox function of apurinic/apyrimidinic endonuclease 1/redox enhancing factor-1 (Ape1/ref-1), *J Med Chem 53*, 1200-1210.
47. Hiramoto, M., Shimizu, N., Nishi, T., Shima, D., Aizawa, S., Tanaka, H., Hatakeyama, M., Kawaguchi, H., and Handa, H. (2002) High-performance affinity beads for identifying anti-NF-kappa B drug receptors, *Methods Enzymol 353*, 81-88.
48. Hiramoto, M., Shimizu, N., Sugimoto, K., Tang, J., Kawakami, Y., Ito, M., Aizawa, S., Tanaka, H., Makino, I., and Handa, H. (1998) Nuclear targeted suppression of NF-kappa B activity by the novel quinone derivative E3330, *J Immunol 160*, 810-819.
49. Bobola, M. S., Finn, L. S., Ellenbogen, R. G., Geyer, J. R., Berger, M. S., Braga, J. M., Meade, E. H., Gross, M. E., and Silber, J. R. (2005) Apurinic/apyrimidinic endonuclease activity is associated with response to radiation and chemotherapy in medulloblastoma and primitive neuroectodermal tumors, *Clin Cancer Res 11*, 7405-7414.
50. Chen, D. S., and Olkowski, Z. L. (1994) Biological responses of human apurinic endonuclease to radiation-induced DNA damage, *Ann N Y Acad Sci 726*, 306-308.
51. Fishel, M. L., He, Y., Reed, A. M., Chin-Sinex, H., Hutchins, G. D., Mendonca, M. S., and Kelley, M. R. (2008) Knockdown of the DNA repair and redox signaling protein Ape1/Ref-1 blocks ovarian cancer cell and tumor growth, *DNA Repair (Amst) 7*, 177-186.
52. Fishel, M. L., He, Y., Smith, M. L., and Kelley, M. R. (2007) Manipulation of base excision repair to sensitize ovarian cancer cells to alkylating agent temozolomide, *Clin Cancer Res 13*, 260-267.
53. Herring, C. J., West, C. M., Wilks, D. P., Davidson, S. E., Hunter, R. D., Berry, P., Forster, G., MacKinnon, J., Rafferty, J. A., Elder, R. H., Hendry, J. H., and Margison, G. P. (1998) Levels of the DNA repair enzyme human apurinic/apyrimidinic endonuclease (APE1, APEX, Ref-1) are associated with the intrinsic radiosensitivity of cervical cancers, *Br J Cancer 78*, 1128-1133.

54. Lau, J. P., Weatherdon, K. L., Skalski, V., and Hedley, D. W. (2004) Effects of gemcitabine on APE/ref-1 endonuclease activity in pancreatic cancer cells, and the therapeutic potential of antisense oligonucleotides, *Br J Cancer 91*, 1166-1173.
55. Ono, Y., Furuta, T., Ohmoto, T., Akiyama, K., and Seki, S. (1994) Stable expression in rat glioma cells of sense and antisense nucleic acids to a human multifunctional DNA repair enzyme, APEX nuclease, *Mutat Res 315*, 55-63.
56. Walker, L. J., Craig, R. B., Harris, A. L., and Hickson, I. D. (1994) A role for the human DNA repair enzyme HAP1 in cellular protection against DNA damaging agents and hypoxic stress, *Nucleic Acids Res 22*, 4884-4889.
57. Wang, D., Luo, M., and Kelley, M. R. (2004) Human apurinic endonuclease 1 (APE1) expression and prognostic significance in osteosarcoma: enhanced sensitivity of osteosarcoma to DNA damaging agents using silencing RNA APE1 expression inhibition, *Mol Cancer Ther 3*, 679-686.
58. Kim, Y. J., Pannell, L. K., and Sackett, D. L. (2004) Mass spectrometric measurement of differential reactivity of cysteine to localize protein-ligand binding sites. Application to tubulin-binding drugs, *Anal Biochem 332*, 376-383.
59. Rishavy, M. A., Pudota, B. N., Hallgren, K. W., Qian, W., Yakubenko, A. V., Song, J. H., Runge, K. W., and Berkner, K. L. (2004) A new model for vitamin K-dependent carboxylation: the catalytic base that deprotonates vitamin K hydroquinone is not Cys but an activated amine, *Proc Natl Acad Sci U S A 101*, 13732-13737.
60. Kurono, S., Kurono, T., Komori, N., Niwayama, S., and Matsumoto, H. (2006) Quantitative proteome analysis using D-labeled N-ethylmaleimide and 13C-labeled iodoacetanilide by matrix-assisted laser desorption/ionization time-of-flight mass spectrometry, *Bioorg Med Chem 14*, 8197-8209.
61. Guan, L., and Kaback, H. R. (2007) Site-directed alkylation of cysteine to test solvent accessibility of membrane proteins, *Nat Protoc 2*, 2012-2017.
62. Zhu, M. M., Rempel, D. L., Du, Z., and Gross, M. L. (2003) Quantification of protein-ligand interactions by mass spectrometry, titration, and H/D exchange: PLIMSTEX., *J. Am. Chem. Soc. 125*, 5252-5253.
63. Zou, G. M., Karikari, C., Kabe, Y., Handa, H., Anders, R. A., and Maitra, A. (2009) The Ape-1/Ref-1 redox antagonist E3330 inhibits the growth of tumor endothelium and endothelial progenitor cells: therapeutic implications in tumor angiogenesis, *J Cell Physiol 219*, 209-218.
64. Kelley, M. R., Luo, M., Reed, A., Su, D., Delaplane, S., Borch, R., Nyland Ii, R. L., Gross, M. L., and Georgiadis, M. (2010) Functional analysis of novel analogs of E3330 that block the redox signaling activity of the multifunctional AP endonuclease/redox signaling enzyme APE1/Ref-1, *Antioxid Redox Signal*.
65. Bapat, A., Fishel, M., and Kelley, M. R. (2009) Going Ape as an Approach to Cancer Therapeutics, *Antioxid Redox Signal 11*, 651-668.

Curriculum Vitae

Sarah Ann Delaplane

Education

Master of Science, Biotechnology (2011)
Indiana University, Indianapolis, IN
Thesis: Mass Spectrometric Approaches to Probing the Redox Function of Ape1

Graduate Certificate in Biotechnology (2005)
Indiana University, Indianapolis, IN

Bachelor of Science, Chemistry (2002)
Butler University, Indianapolis, IN

Professional Experience

Research Technician, Department of Biochemistry/Molecular Biology Indiana University, Indianapolis, IN, 2003-2011

Biochemical research in an X-ray

- Independently optimize experimental conditions
- Lab maintenance including ordering and receiving supplies

Research Experience

Protein Purification

- Large scale purification of recombinant proteins using French press, ultra centrifugation, and an AKTA FPLC.
- Protein purification with tagged proteins using gel filtration, and separation by ion exchange and size exclusion chromatography.

Mass Spectrometry

- Experience on Perkin Elmer prO-TOF, Finnigan LTQ FT, and MicroMass Q-TOF Ultima Global
- Use of appropriate software for data analysis

Development of High-Throughput Screen

- Development of high-throughput screen of a 60K commercially available library of compounds for inhibition of enzymatic activity.
- Z' analysis of 384 well plates for screen viability using positive and negative controls.

Crystallization of Protein

- Hanging-drop vapor crystallization

Addition Skills

- Cloning and PCR mutagenesis including primer design
- DNA isolation and transformation
- Purification of DNA oligos by HPLC
- SDS-PAGE
- Preparation of media, reagents, competent cells, chromatography columns, acrylamide and agarose gels

Publications

1) Luo, M., Delaplane, S., Jiang, A., Reed, A., He, Y., Fishel, M., Nyland II, R. L., Borch, R. F., Qiao, X., Georgiadis, M. M., and Kelley, M. R. (2008) Role of the multifunctional DNA repair and redox signaling protein Ape1/Ref-1 in cancer and endothelial cells: Small molecule inhibition of Ape1's redox function, *Antioxid Redox Signal 10*, 1853-1867.

2) Georgiadis, M. M., Luo, M., Gaur, R. K., Delaplane, S., Li, X., and Kelley, M. R. (2008) Evolution of the redox function in mammalian apurinic/apyrimidinic endonuclease, *Mutat Res 643*, 54-63.

3) Su, D., Delaplane, S., Luo, M., Rempel, D. L., Vu, B., Kelley, M. R., Gross, M. L., and Georgiadis, M. M. (2011) Interactions of Apurinic/Apyrimidinic Endonuclease with a Redox Inhibitor: Evidence for an Alternate Conformation of the Enzyme, *Biochemistry 50*, 82-92.

4) Kelley, M. R., Luo, M., Reed, A., Su, D., Delaplane, S., Borch, R. F., Nyland, R. L., Gross, M. L., and Georgiadis, M. M. (2011) Functional Analysis of Novel Analogues of E3330 That Block the Redox Signaling Activity of the Multifunctional AP Endonuclease/Redox Signaling Enzyme APE1/Ref-1, *Antioxid Redox Signal 14*, 1387-1401.

5) Onyango, D., Naguleswaran, A., Delaplane, S., Reed, A., Kelley, M., Georgiadis, M., Sullivan, W. (2011) Base Excision Repair Apurinic/Apyrimidinic Endonucleases in Apicomplexan Parasite Toxoplasma Gondii, *DNA Repair 10*, 466-75.